NACA RM L51K16

NACA

RESEARCH MEMORANDUM

FREE-FLIGHT MEASUREMENTS OF SOME EFFECTS OF AILERON SPAN, CHORD, AND DEFLECTION AND OF WING FLEXIBILITY ON THE ROLLING EFFECTIVENESS OF AILERONS ON SWEPTBACK WINGS AT MACH NUMBERS BETWEEN 0.8 AND 1.6

By Eugene D. Schult, H. Kurt Strass, and E. M. Fields

Langley Aeronautical Laboratory
Langley Field, Va.

NATIONAL ADVISORY COMMITTEE
FOR AERONAUTICS

WASHINGTON
January 24, 1952

NATIONAL ADVISORY COMMITTEE FOR AERONAUTICS

RESEARCH MEMORANDUM

FREE-FLIGHT MEASUREMENTS OF SOME EFFECTS OF AILERON SPAN, CHORD, AND DEFLECTION AND OF WING FLEXIBILITY ON THE ROLLING EFFECTIVENESS OF AILERONS ON SWEPTBACK WINGS AT MACH NUMBERS BETWEEN 0.8 AND 1.6

By Eugene D. Schult, H. Kurt Strass, and E. M. Fields

SUMMARY

As part of the NACA transonic research program, a free-flight investigation has been made by the Pilotless Aircraft Research Division to determine some effects of aileron span and deflection on the rolling effectiveness of plain, sealed, 15-percent- and 30-percent-chord flap-type ailerons through the Mach number range of 0.8 to 1.6. The wings had quarter-chord lines swept back 35° and 45°, aspect ratios of 4.0, taper ratios of 0.6, and NACA 65A006 airfoil sections parallel to the free stream. Wings of different degrees of torsional flexibility were tested and the results extended to estimate the rigid-wing rolling effectiveness of all aileron configurations tested.

The results of this investigation indicate that the maximum unit-aileron rolling effectiveness for a 45° sweptback wing occurs at approximately the mid-exposed-semispan station. The 15-percent-chord full-span ailerons were approximately two-thirds as effective in rolling power as the 30-percent-chord ailerons on 45° sweptback wings over the Mach number range tested. The advantage in rolling effectiveness gained by using the larger aileron-chord ratio became insignificant for $0.43\frac{b}{2}$ - span outboard ailerons at supersonic speeds and for $0.215\frac{b}{2}$ - span outboard ailerons throughout the Mach number range. These results indicate that for a given outboard aileron there exists an optimum aileron-chord ratio which decreases with decreasing aileron span. The variation of rolling effectiveness with control deflection for the 35° sweptback wings was essentially linear over the range of deflections and Mach numbers tested; increasing the wing sweepback to 45° resulted in a slightly decreasing rate of change of rolling effectiveness with increasing deflections at supersonic speeds. Increasing the angle of wing sweepback from 35° to

45° also resulted in higher rolling-effectiveness values at transonic speeds and removed the abrupt changes in the variation of $pb/2V$ with Mach number observed near Mach number 1.0 for the 35° sweptback configurations.

INTRODUCTION

As part of the NACA transonic research program, the Langley Pilotless Aircraft Research Division has conducted experimental investigations to determine the rolling effectiveness of plain, true-contour, flap-type ailerons on thin, tapered, sweptback wings over an extreme Mach number range of approximately 0.7 to 1.8. These data were obtained with rocket-propelled test vehicles in free flight by means of the technique described in reference 1. Results were obtained on wings having the quarter-chord lines swept back 35° and 45°, aspect ratios of 4.0, taper ratios of 0.6, and NACA 65A006 airfoil sections parallel to the free stream. Some effects of aileron span and location on rolling effectiveness were determined for 30-percent-chord ailerons on both 35° and 45° sweptback wings and for 15-percent-chord ailerons on the 45° sweptback wings. Included in the data for the configurations with 30-percent-chord ailerons are some experimental aeroelastic effects of wing torsional flexibility on rolling effectiveness; these data were used to estimate the rigid-wing rolling effectiveness of all aileron configurations.

This paper also presents rolling-effectiveness data calculated from results of tests made on similar wing-aileron configurations in the Langley high-speed 7- by 10-foot tunnel and reported in references 2 and 3.

SYMBOLS

A	aspect ratio $\left(\frac{b^2}{S} = 4.0\right)$
b	diameter of circle swept by wing tips, 3.0 feet
S	area of two wings measured to model center line, 2.25 square feet
c	local chord, feet
c_{av}	average exposed wing chord parallel to model center line, 0.72 foot

c_t	wing chord at tip, parallel to model center line, 0.56 foot
c_r	wing chord at, and parallel to, model center line, 0.94 foot
M	Mach number
P	static pressure, pounds per square foot
p	rolling velocity, positive if model is rolling clockwise when viewed from rear, radians per second
q	dynamic pressure, pounds per square foot
V	flight-path velocity, feet per second
R	Reynolds number of tests, based on c_{av}
pb/2V	wing-tip helix angle, radians
δ	deflection of one aileron measured in a plane normal to wing-chord plane and perpendicular to hinge line (positive down when wing is on left), average for three wings, degrees
α	angle of attack of wings with respect to free stream, degrees
i_w	average incidence per wing for three wings measured in a plane normal to wing-chord plane and parallel to free-stream, positive if tending to produce clockwise roll when viewed from rear, degrees
y	spanwise ordinate, measured from and normal to model center line, feet
λ	taper ratio $\left(\frac{c_t}{c_r} = 0.6\right)$
$\Lambda_{c/4}$	angle of sweepback of quarter-chord line, degrees
τ	derived constant for wing and aileron (see references 4 and 5)
ϕ	fraction of rigid-wing rolling effectiveness retained by flexible wing

m concentrated couple, applied near wing tip in a plane parallel to free stream and normal to wing-chord plane, foot-pounds

θ angle of twist produced by m at any section along wing span in a plane parallel to free stream and normal to wing-chord plane, radians

r reference aileron station (mid-aileron) parallel to free stream, measured normal to model center line from fuselage, inches

$(\theta/m)_r$ wing torsional-flexibility parameter measured at mid-aileron in a plane parallel to free stream and normal to wing-chord plane, radians per foot-pound

P_a/P_o ratio of static pressure at test altitude to standard static pressure at sea level

C_l rolling-moment coefficient for two wings $\left(\frac{\text{Rolling moment}}{qSb}\right)$

$\frac{c_m/\delta}{\alpha/\delta}$ effective section twisting-moment parameter for constant lift (see reference 4), per radian

$$C_{l_\delta} = \left(\frac{\partial C_l}{\partial \delta}\right)_{\alpha=0}$$

$$C_{l_p} = \left(\frac{\partial C_l}{\partial (pb/2V)}\right)_{\alpha=0}$$

Subscripts:

a altitude, or aileron when used in conjunction with chord

o sea level, or outboard when used in conjunction with aileron span

i inboard when used in conjunction with aileron span

R rigid

F flexible

MODELS AND TECHNIQUE

Typical test vehicles of the type used in the present investigation are illustrated in the photographs presented as figure 1. The test wings had quarter-chord lines swept back 35° and 45°, respectively, aspect ratios of 4.0, taper ratios of 0.6, and NACA 65A006 airfoil sections parallel to the free stream. A complete description of the test vehicles is given in table I and figure 2. Various control deflections were tested for the 30-percent-chord outboard ailerons of 0.86b/2 span and 0.43b/2 span on both 35° and 45° sweptback wing configurations. All other aileron configurations were preset at an angle of approximately 5°. Four wing-aileron combinations having 30-percent-chord ailerons and wings with different degrees of torsional flexibility were tested to determine some aeroelastic effects of wing twist on rolling effectiveness. These four combinations included 35° sweptback wings having $0.43\frac{b}{2}$ - span outboard ailerons, and 45° sweptback wings having $0.43\frac{b}{2}$ - span and $0.86\frac{b}{2}$ - span outboard and $0.43\frac{b}{2}$ - span inboard ailerons. Measured values of the wing torsional-flexibility parameter θ/m, plotted as a function of distance from fuselage, are shown in figure 3.

The flight tests were made at the Pilotless Aircraft Research Station at Wallops Island, Va. The test vehicles were propelled by a two-stage rocket propulsion system to a Mach number of about 1.6. During a period of approximately 10 seconds of coasting flight following rocket-motor burnout, time-history measurements were made of the flight-path velocity with CW Doppler radar and of rolling velocity with special spinsonde radio equipment. These data in conjunction with atmospheric data obtained with radiosondes permit the evaluation of the wing-aileron rolling effectiveness in terms of the parameter $pb/2V$ as a function of Mach number. Reference 1 gives a more complete description of the flight-testing technique.

The Reynolds number varied from approximately 2×10^6 to 8×10^6 over the Mach number range (see fig. 4).

ACCURACY

From previous experience and mathematical analysis, the experimental uncertainties are believed to be within the following limits:

	Subsonic	Supersonic
M	±0.010	±0.005
$(pb/2V)_F$	±0.005	±0.003
$(pb/2V)_R$	±0.007	±0.005

The sensitivity of the experimental technique is such, however, that small irregularities in the variation of $pb/2V$ with Mach number (of about half the magnitude shown in the table) may be detected. The maximum uncertainties in the determination of i_w and δ are $\pm 0.05^\circ$ and $\pm 0.10^\circ$, respectively.

CORRECTIONS

Aeroelasticity

Rigid-wing rolling-effectiveness values were estimated from flexible-wing data by the method of reference 4, using the relations from reference 4:

$$(1 - \phi)_o = \frac{c_m/\delta}{\alpha/\delta} \tau \frac{b^3}{2A^2} q_o (\theta/m)_r \qquad (1)$$

and reference 6:

$$(1 - \phi)_a = \frac{P_a}{P_o}(1 - \phi)_o \qquad (2)$$

where $(1 - \phi)_o$ is the fraction of rigid-wing rolling effectiveness lost by the flexible wing at sea level, $\frac{c_m/\delta}{\alpha/\delta}$ is the section twisting-moment parameter for constant lift, τ is an aeroelastic weighing factor derived in reference 4 but corrected for aspect ratio, taper ratio, and wing sweep in reference 5 (see table II), q_o is standard sea-level dynamic pressure, and $(\theta/m)_r$ is the wing torsional-flexibility parameter at the mid-aileron reference station (fig. 3). The fraction of rigid-wing rolling effectiveness lost by wing twist was determined for a particular wing-aileron configuration by flying several test vehicles differing in degrees of wing torsional flexibility. From results of the flight tests

of these models it was possible to solve equations (1) and (2) over the Mach number range for $\frac{c_{m_\delta}}{c_{\alpha_\delta}}$. These $\frac{c_{m_\delta}}{c_{\alpha_\delta}}$ values were then used to correct $(pb/2V)_{F_a}$ data for similar ailerons with different deflections to rigid-wing rolling effectiveness. A more detailed description of this method of deriving rigid-wing rolling effectiveness from flexible-wing data can be found in reference 6.

Aileron Deflection

In the evaluation of the aeroelastic effects of wing twist, slight differences in rolling effectiveness due to small differences in control deflection of the order of 0.5° between several models of a given aileron configuration (see table I) were taken into account by correcting the $(pb/2V)_{F_a}$ data to correspond to the deflection of the most flexible wing configuration. This correction was accomplished by assuming a linear variation of rolling effectiveness with aileron deflection.

Wing Incidence

Measured values of $(pb/2V)_{F_a}$ were corrected to values corresponding to zero incidence by the following equation from reference 7:

$$\Delta(pb/2V) = \frac{2i_w}{57.3}\frac{1 + 2\lambda}{1 + 3\lambda} \tag{3}$$

where $\Delta(pb/2V)$ is the increment of $pb/2V$ due to wing incidence i_w. Table I lists values of i_w measured before flight.

Inertia

Calculations (see reference 1) indicate that the effects of test-vehicle inertia effects about the roll axis were small, being of the order of 3 percent near Mach number 1.

RESULTS AND DISCUSSION

The results of this investigation are presented in figures 5 to 16. All rolling-effectiveness data except the basic data plotted in figures 5 and 6 have been corrected to rigid-wing values by the method of references 4 and 6.

The basic-data plots of the flexible-wing rolling-effectiveness parameter $(pb/2V)_{F_a}$ and of the static-pressure ratio P_a/P_o are presented as functions of Mach number in figure 5 for the 35° sweptback wing configurations and in figure 6 for the 45° sweptback wing configurations. These values of $(pb/2V)_{F_a}$ were corrected to correspond to $i_w = 0°$ but were uncorrected for differences in altitude.

Experimentally derived values of the effective twisting-moment parameter $\frac{c_m/\delta}{\alpha/\delta}$ were evaluated from the flexible-wing data and are shown in figure 7 plotted as a function of Mach number for 0.30-chord outboard ailerons having spans of 0.43b/2 for the 35° sweptback wing, and spans of 0.86b/2 and 0.43b/2 for the 45° sweptback wing configurations. Experimental values of $\frac{c_m/\delta}{\alpha/\delta}$ were also obtained for the 0.30-chord inboard aileron configuration with 0.43b/2 span on the 45° sweptback wing. The extent of experimental data on model 4 (fig. 5) limited a straightforward determination of the parameter $\frac{c_m/\delta}{\alpha/\delta}$ for the $0.43\frac{b}{2}$ - span outboard aileron on the 35° sweptback wing to Mach numbers less than 1.1. Approximate values of $\frac{c_m/\delta}{\alpha/\delta}$ were obtained at higher Mach numbers by utilizing $(pb/2V)_F$ data from models 5, 6, and 7 and assuming a linear variation of rolling effectiveness with control deflection to determine $(pb/2V)_F$ data at a deflection of 10.2°. Small differences in altitude of these models were taken into account. For 0.15-chord ailerons the variation of $\frac{c_m/\delta}{\alpha/\delta}$ with Mach number was estimated at subsonic speeds, using values of $\frac{c_m/\delta}{\alpha/\delta}$ for 0.30-chord ailerons in conjunction with experimental results reported in reference 8 on the variation of pitching-moment coefficient

with aileron-chord ratio. At supersonic speeds $\frac{c_m/\delta}{\alpha/\delta}$ was assumed to vary linearly with aileron-chord ratio on the basis of linearized theory.

Effect of Aileron Deflection on Rolling Effectiveness

The rolling effectiveness (corrected to rigid-wing values) of 0.30-chord outboard ailerons with spans of 0.86b/2 and 0.43b/2 is presented in figure 8 for 35° sweptback wings and in figure 9 for 45° sweptback wings. The $(pb/2V)_R$ data shown for the full-span aileron on the 35° sweptback wing were obtained by using values of $\frac{c_m/\delta}{\alpha/\delta}$ for the full-span aileron on the 45° sweptback wing; the possible error in $(pb/2V)_R$ caused by this substitution is believed to be small and to lie within the experimental error.

Results show that for 35° sweptback wings, aileron rolling effectiveness is essentially linear with control deflection over the range of deflections and Mach numbers tested. Increasing the wing sweepback to 45° did not affect the linearity of rolling effectiveness with control deflection at high subsonic speeds but induced a tendency toward a reduced rate of change of rolling effectiveness with increasing deflection at supersonic speeds.

Effect of Aileron Span and Spanwise Location

Since rolling effectiveness is essentially linear with control deflection for deflections up to 5°, the rolling effectiveness of the various aileron configurations is reduced to the form $\frac{(pb/2V)_R}{\delta}$, where the values of $(pb/2V)_R$ are selected to correspond to a control deflection of approximately 5°. Figure 10 shows for 0.30-chord ailerons on a 35° sweptback wing that $0.43\frac{b}{2}$ - span outboard ailerons have approximately half the rolling effectiveness of $0.86\frac{b}{2}$ - span ailerons throughout the Mach number range. The Mach number at which the abrupt change in slope of the variation of rolling effectiveness with Mach number occurs is slightly lower for the full-span aileron (M = 0.92) than for the partial-span aileron (M = 0.96).

Figure 11 presents the variation of rolling effectiveness with Mach number for 45° sweptback wings having outboard ailerons with chord ratios

of 0.15 and 0.30. Twisting-moment parameters were not evaluated experimentally for the $0.215\frac{b}{2}$ - span or the $0.645\frac{b}{2}$ - span outboard ailerons. Therefore, to correct the $0.215\frac{b}{2}$ - span aileron configuration for losses in rolling effectiveness due to wing flexibility, values of $\frac{c_{m_\delta}}{\alpha_\delta}$ for the geometrically closest aileron configuration $\left(0.43\frac{b}{2}\text{ - span outboard}\right)$ were arbitrarily used; rough calculations from tunnel data indicate that this assumption will result in values of $(pb/2V)_R$ which are slightly low but within the experimental error. For the $0.645\frac{b}{2}$ - span aileron configuration a curve of $\frac{c_{m_\delta}}{\alpha_\delta}$ as a function of Mach number was averaged from $0.43\frac{b}{2}$ - span and $0.86\frac{b}{2}$ - span outboard-aileron data (45° sweptback wing); this average is believed to represent a close approximation of the twisting-moment parameter for the $0.645\frac{b}{2}$ - span aileron configuration. The possible errors in $(pb/2V)_R$ resulting from these assumptions are estimated to be small for the range of wing flexibilities considered in figure 11; for example, an arbitrary 10-percent increment in the value of $\frac{c_{m_\delta}}{\alpha_\delta}$ for the $0.43\frac{b}{2}$ - span aileron (fig. 7) will result in an increment in the final value of $(pb/2V)_R$ of approximately 3 percent near Mach number 1.0 and 5 percent near Mach number 1.6.

Examination of figure 11 indicates that the variation of rigid-wing rolling effectiveness with Mach number is affected considerably by aileron span and aileron chord ratio. In figure 12 the variation of rolling effectiveness with outboard aileron span is indicated for different Mach numbers. The slopes of these curves, which indicate the rate of change of rolling effectiveness per unit aileron span, show that the maximum unit-aileron rolling effectiveness for the 45° sweptback wing occurs at approximately the mid-exposed-semispan station for the 30-percent chord ailerons and between the mid-exposed-semispan station and the tip for 15-percent chord ailerons. Similar cross plots using rolling-effectiveness data uncorrected for losses due to wing flexibility showed no apparent change in the above-mentioned optimum unit-aileron locations.

Three configurations were tested to determine the utility of figure 12 in predicting the rolling effectiveness of other than outboard aileron configurations; two configurations had $0.215\frac{b}{2}$ - span centrally located ailerons with chord ratios of 0.15 and 0.30 respectively, and the

third had $0.43\frac{b}{2}$ - span inboard ailerons with a chord ratio of 0.30. Measured results in figure 13 compared favorably with rolling-effectiveness values estimated from figure 12 except for the inboard aileron configuration which yielded higher measured results at transonic speeds.

Figure 14 shows the fraction of the rigid-wing rolling effectiveness at Mach number 0.80 retained over the Mach number range for different ailerons on 45° sweptback wings. Results indicate that the least percentage decrease in rolling effectiveness over the Mach number range of 0.80 to 1.60 was experienced by the 15-percent-chord, $0.43\frac{b}{2}$ - span outboard aileron configuration. The figure also indicates for 30-percent-chord ailerons that the percentage of the rolling effectiveness at $M = 0.80$ retained over the transonic range generally increases as the mid-aileron reference station approaches the wing root; this effect is less well defined for 15-percent-chord ailerons.

Effect of Aileron-Chord Ratio

In figure 15 the variation of rolling effectiveness with Mach number of 15-percent- and 30-percent-chord ailerons on a 45° sweptback wing are compared for various aileron spans. Results show that 15-percent-chord full-span ailerons are approximately two-thirds as effective in rolling power as 30-percent-chord ailerons over the Mach number range tested. The advantage in rolling effectiveness gained by using the larger aileron-chord ratio became insignificant for $0.43\frac{b}{2}$ - span outboard ailerons at supersonic speeds and for $0.215\frac{b}{2}$ - span outboard ailerons throughout the Mach number range. This indicates that for a given outboard aileron there exists an optimum aileron-chord ratio which decreases with decreasing aileron span.

Effect of Sweepback

Figure 16 compares the variation of rolling effectiveness with Mach number for $0.43\frac{b}{2}$ - span and $0.86\frac{b}{2}$ - span outboard ailerons on 35° and 45° sweptback wings. Generally, the 35° sweptback configurations had more rolling effectiveness at high subsonic speeds and at Mach numbers greater than 1.20, but more abrupt changes in the variation of $(pb/2V)_R$ with Mach number through the transonic range, than the 45° sweptback configurations.

Comparison of Results

Figure 17 presents as a function of Mach number a comparison of present test $(pb/2V)_R$ data with rolling-effectiveness values derived from the sources indicated on the figure by means of the relationship

$$\frac{pb/2V}{\delta} = \frac{(-)C_{l_\delta}}{C_{l_p}} \tag{4}$$

which for this analysis assumes that the effects of rolling on C_{l_δ} are negligible. The damping-in-roll derivatives from reference 9 were obtained in the Langley high-speed 7- by 10-foot tunnel by the transonic-bump method, utilizing the twisted-wing technique. Rocket-model damping-in-roll derivatives (reference 10) were evaluated from wing-body configurations similar to the present test vehicles but without ailerons. The reference data were not corrected for any twisting or deflection of the wing caused by air loads, but these effects were believed to be small. The symbols on figure 17(b) denote values of $(pb/2V)_F$ obtained in the Langley 300 MPH 7- by 10-foot tunnel on two rocket vehicles having 30-percent-chord, $0.86\frac{b}{2}$ - span and $0.43\frac{b}{2}$ - span outboard ailerons with control deflections of 9.6° and 9.5°, respectively. Because of the low Mach number at which the tunnel tests were conducted, these pb/2V points may be assumed to represent essentially rigid-wing values. No high-speed data were obtained from these models in subsequent flight tests.

Comparison of results in figure 17 shows for the 35° sweptback wing configurations that estimated rigid-wing rolling-effectiveness values from the present investigation were in fair agreement quantitively with pb/2V derived from referenced data by use of equation (4); for the 45° sweptback wing configurations present test results were generally higher throughout the Mach number range. In the variation of pb/2V with Mach number, the results of the present investigation show slightly different trends near and above Mach number 1.0 than those of the referenced Langley 7- by 10-foot tunnel data; the difference in these trends becomes more apparent as the span of the outboard ailerons is increased and is especially pronounced for the inboard $0.43\frac{b}{2}$ - span ailerons on the 45° sweptback wing.

CONCLUSIONS

A free-flight investigation employing the rocket-model technique was made at Mach numbers from 0.8 to 1.6 to determine some effects of aileron span, chord, and deflection on the estimated rigid-wing rolling effectiveness of various flap-type ailerons attached to wings having quarter-chord lines swept back 35° and 45°, aspect ratios of 4.0, taper ratios of 0.6, and NACA 65A006 airfoil sections. From these results the following conclusions can be drawn:

1. The maximum unit-aileron rolling effectiveness for the 45° sweptback wing occurred at approximately the mid-exposed-semispan station for the 30-percent-chord ailerons and between the mid-exposed-semispan station and the tip for 15-percent-chord ailerons.

2. The percentage of the rolling effectiveness at Mach number 0.8 retained by the 30-percent-chord ailerons on 45° sweptback wings over the transonic speed range generally increased as the mid-aileron reference station approached the wing root. This effect was less well defined for the 15-percent-chord ailerons.

3. For 45° sweptback wings the 15-percent-chord full-span ailerons were approximately two-thirds as effective in rolling power as the 30-percent-chord ailerons over the Mach number range tested. The advantage in rolling effectiveness gained by using the larger aileron-chord ratio became insignificant for $0.43\frac{b}{2}$ - span outboard ailerons at supersonic speeds and for $0.215\frac{b}{2}$ - span outboard ailerons throughout the Mach number range. These results indicate that for a given outboard aileron there exists an optimum aileron-chord ratio which decreases with decreasing aileron span.

4. The variation of estimated rigid-wing rolling effectiveness with control deflection for 35° sweptback wings was essentially linear with control deflection for the full-span and the $0.43\frac{b}{2}$ - span outboard ailerons over the range of control deflections tested. Increasing the wing sweepback from 35° to 45° resulted in a slightly decreasing rate of change of rolling effectiveness with increasing deflections at supersonic speeds. Increasing the wing sweepback from 35° to 45° also resulted in higher rolling effectiveness at transonic speeds and removed the abrupt changes

in the variation of $pb/2V$ with Mach number observed near Mach number 1.0 for the 35° sweptback wing configurations.

Langley Aeronautical Laboratory
National Advisory Committee for Aeronautics
Langley Field, Va.

REFERENCES

1. Sandahl, Carl A., and Marino, Alfred A.: Free-Flight Investigation of Control Effectiveness of Full-Span 0.2-Chord Plain Ailerons at High Subsonic, Transonic, and Supersonic Speeds to Determine Some Effects of Section Thickness and Wing Sweepback. NACA RM L7D02, 1947.

2. Thompson, Robert F.: Lateral-Control Investigation of Flap-Type Controls on a Wing with Quarter-Chord Line Swept Back 35°, Aspect Ratio 4, Taper Ratio 0.6, and NACA 65A006 Airfoil Section. Transonic-Bump Method. NACA RM L9L12a, 1950.

3. Vogler, Raymond D.: Lateral-Control Investigation of Flap-Type Controls on a Wing with Quarter-Chord Line Swept Back 45°, Aspect Ratio 4, Taper Ratio 0.6, and NACA 65A006 Airfoil Section. Transonic-Bump Method. NACA RM L9F29a, 1949.

4. Pearson, Henry A., and Aiken, William S., Jr.: Charts for the Determination of Wing Torsional Stiffness Required for Specified Rolling Characteristics or Aileron Reversal Speed. NACA Rep. 799, 1944. (Formerly NACA ACR L4L13.)

5. Strass, H. Kurt: Summary of Some Effective Aerodynamic Twisting-Moment Coefficients of Various Wing-Control Configurations at Mach Numbers from 0.6 to 1.7 as Determined from Rocket-Powered Models. NACA RM L51K20, 1952.

6. Strass, H. Kurt, Fields, E. M., and Purser, Paul E.: Experimental Determination of Effect of Structural Rigidity on Rolling Effectiveness of Some Straight and Swept Wings at Mach Numbers from 0.7 to 1.7. NACA RM L50G14b, 1950.

7. Strass, H. Kurt, and Marley, Edward T.: Rolling Effectiveness of All-Movable Wings at Small Angles of Incidence at Mach Numbers from 0.6 to 1.6. NACA RM L51H03, 1951.

8. Langley Research Staff (Compiled by Thomas A. Toll): Summary of Lateral-Control Research. NACA Rep. 868, 1947. (Formerly NACA TN 1245.)

9. Lockwood, Vernard E.: Effects of Sweep on the Damping-in-Roll Characteristics of Three Sweptback Wings Having an Aspect Ratio of 4 at Transonic Speeds. NACA RM L50J19, 1950.

10. Sanders, E. Claude, Jr., and Edmondson, James L.: Damping in Roll of Rocket-Powered Test Vehicles Having Swept, Tapered Wings of Low Aspect Ratio. NACA RM L51G06, 1951.

11. Kuhn, Richard E., and Myers, Boyd C., II: Effects of Mach Number and Sweep on the Damping-in-Roll Characteristics of Wings of Aspect Ratio 4. NACA RM L9E10, 1949.

TABLE I.- GEOMETRIC CHARACTERISTICS OF TEST WINGS

Model	$\Lambda_{c/4}$ (deg)	Aileron span	$2y_o/b$	c_a/c (1)	δ_a (deg)	i_w (deg)	Wing construction (2)
1	35	0.86b/2	1.00	0.30	10.02	-0.01	2
2	35	.86b/2	1.00	.30	5.05	-.01	1
3	35	.86b/2	1.00	.30	1.76	-.07	1
4	35	.43b/2	1.00	.30	10.20	.05	1
5	35	.43b/2	1.00	.30	4.70	.06	1
6	35	.43b/2	1.00	.30	4.54	.08	1
7	35	.43b/2	1.00	.30	2.05	-.03	1
8	35	.43b/2	1.00	.30	9.96	-.02	3
9	45	.86b/2	1.00	.30	4.94	-.03	2
10	45	.86b/2	1.00	.30	2.06	-.05	1
11	45	.86b/2	1.00	.30	5.07	-.01	3
12	45	.645b/2	1.00	.30	4.79	.09	2
13	45	.43b/2	1.00	.30	18.76	.01	1
14	45	.43b/2	1.00	.30	10.14	-.04	2
15	45	.43b/2	1.00	.30	5.05	.01	1
16	45	.43b/2	1.00	.30	4.97	.01	2
17	45	.43b/2	1.00	.30	1.89	.04	1
18	45	.43b/2	1.00	.30	9.92	0	3
19	45	.215b/2	1.00	.30	4.86	.07	2
20	45	.43b/2	.57	.30	4.96	-.04	2
21	45	.43b/2	.57	.30	4.98	-.08	3
22	45	.215b/2	.57	.30	5.00	-.04	2
23	45	.86b/2	1.00	.15	5.54	-.10	2
24	45	.645b/2	1.00	.15	5.26	.01	2
25	45	.43b/2	1.00	.15	5.28	-.06	2
26	45	.215b/2	1.00	.15	5.09	-.07	2
27	45	.215b/2	.57	.15	4.68	.08	2

[1]Based upon streamwise chord.

[2]1. Solid duralumin
2. Spruce with 0.040-inch-thick steel inlay and 0.125-inch-thick aluminum alloy chord-plane stiffener
3. Spruce with 0.125-inch-thick aluminum-alloy chord-plane stiffener

TABLE II.- LIST OF DERIVED VALUES OF THE CONSTANT τ[1]

$\Lambda_{c/4}$ (deg)	Aileron span	$\frac{y_i}{b/2}$	$\frac{y_o}{b/2}$	τ
35	0.43b/2	0.570	1.00	0.260
35	.86b/2	.140	1.00	.520
45	.215b/2	.785	1.00	.220
45	.43b/2	.570	1.00	.260
45	.645b/2	.355	1.00	.340
45	.86b/2	.140	1.00	.510
45	.43b/2	.140	.57	1.170
45	.215b/2	.355	.57	.670

[1]From reference 5.

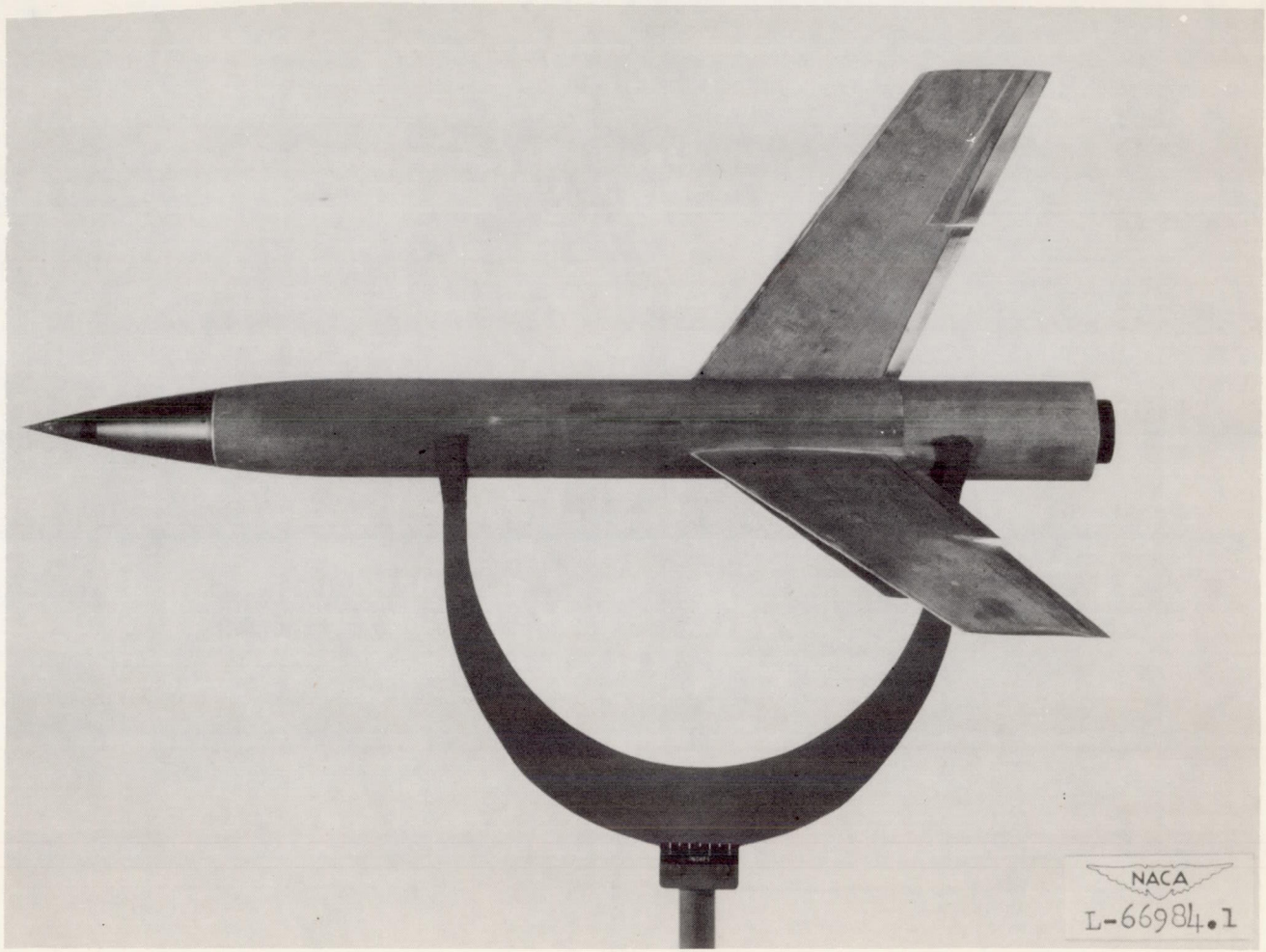

(a) 35° sweptback wing.

Figure 1.- Typical test vehicles.

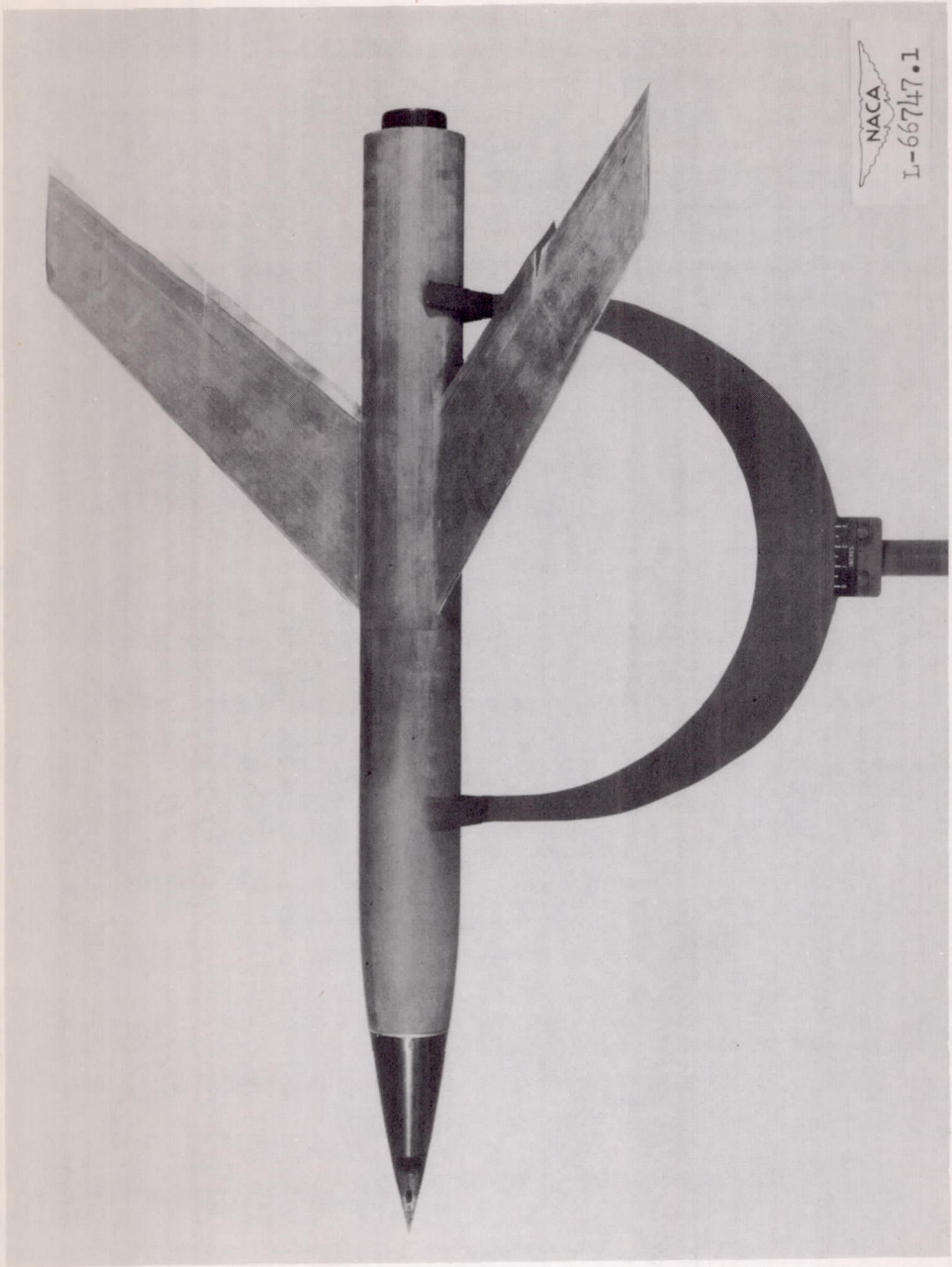

(b) 45° sweptback wing.

Figure 1.- Concluded.

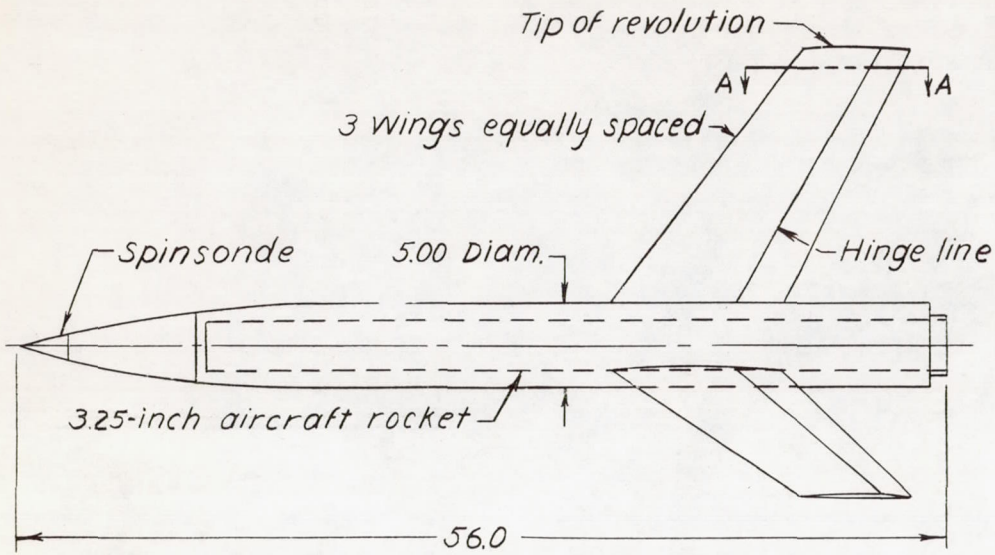

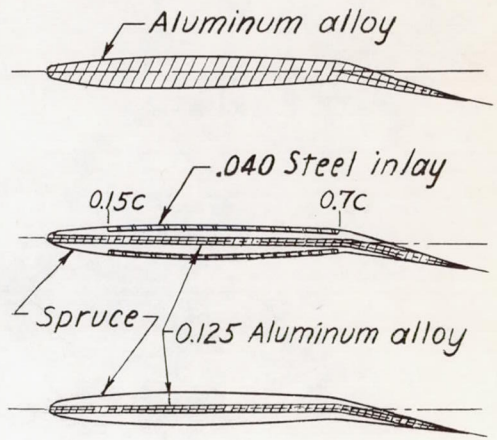

Typical Section A-A

Types of wing structure employed

TABULATED WING DATA

Aspect ratio ____ 4.0	Area (3 semispans) __ 485 sq in.
Taper ratio ____ 0.6	Span (Twice semispan) __ 36.00 in.
Sweepback, c/4 __ 35°, 45°	Chord at tip _____ 6.74 in.
Section __ NACA 65A006	Chord at centerline __ 11.24 in.

(a) Test vehicle and wing details. All dimensions are in inches.

Figure 2.- General arrangement of test vehicles.

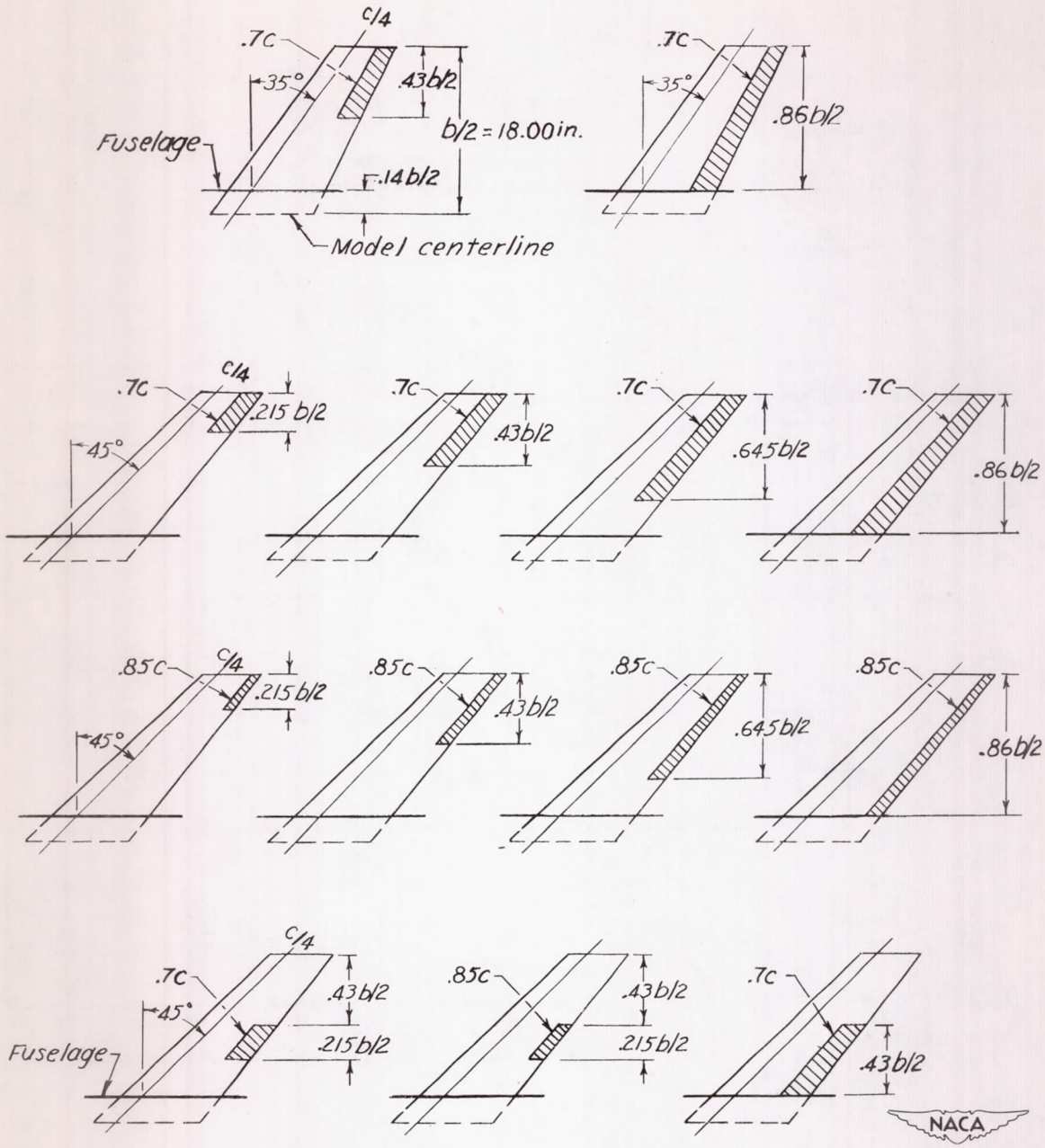

(b) Wing-aileron configurations tested.

Figure 2.- Concluded.

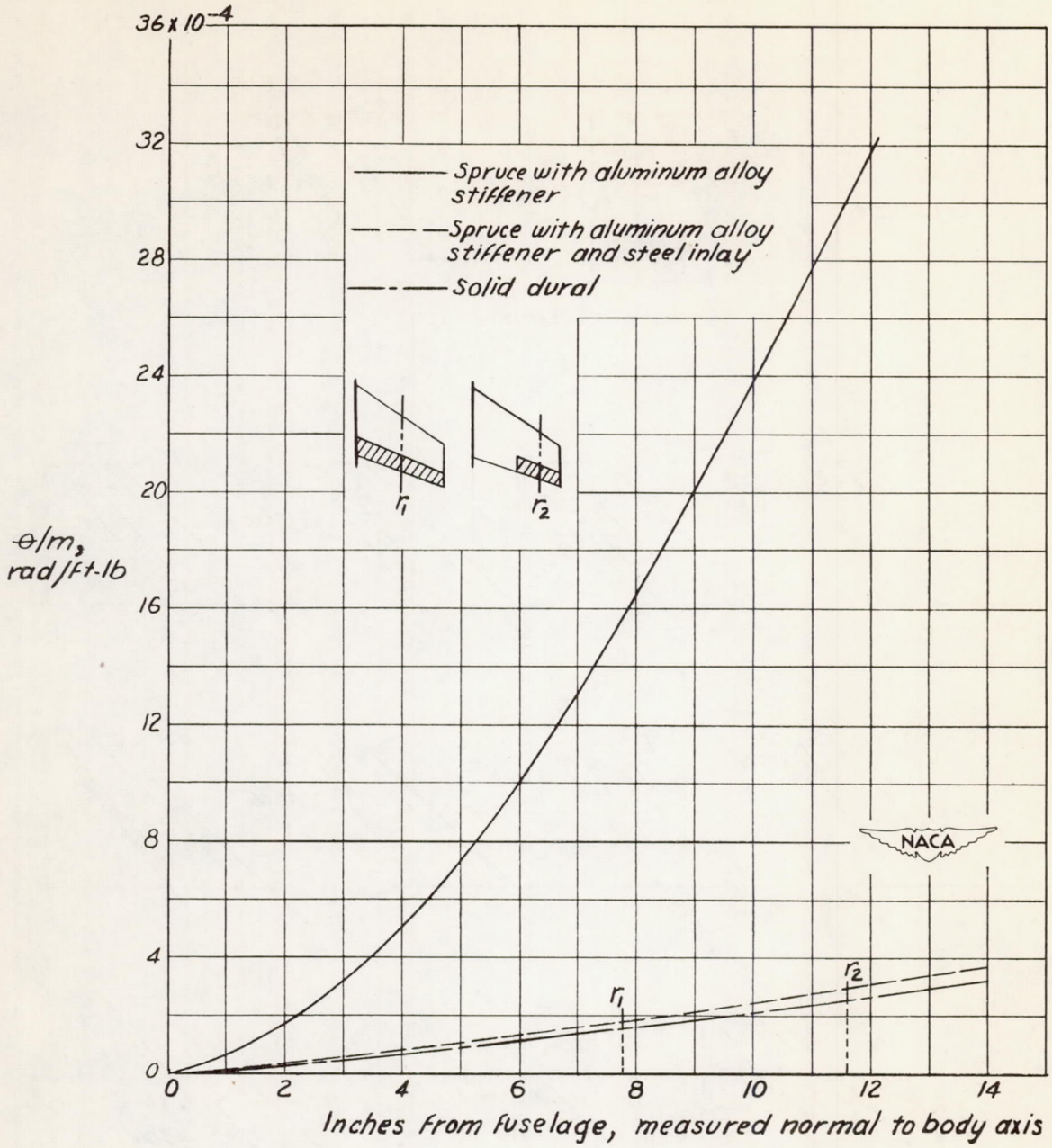

(a) $\Lambda_{c/4} = 35^{\circ}$.

Figure 3.- Spanwise variation of wing torsional-flexibility parameter. Couple applied at wing tip in a plane normal to wing-chord plane and parallel to body axis.

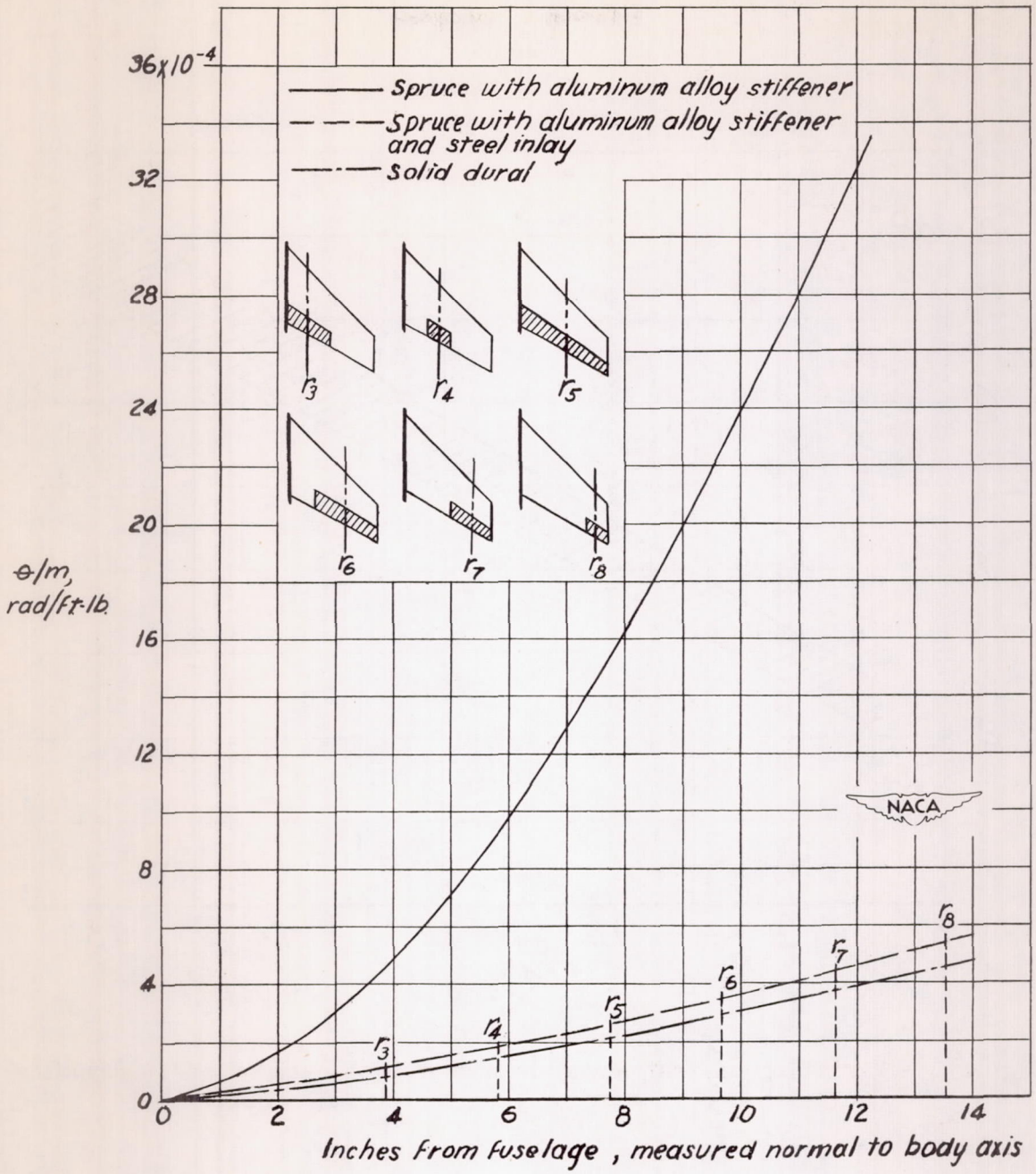

(b) $\Lambda_{c/4} = 45^{\circ}$.

Figure 3.- Concluded.

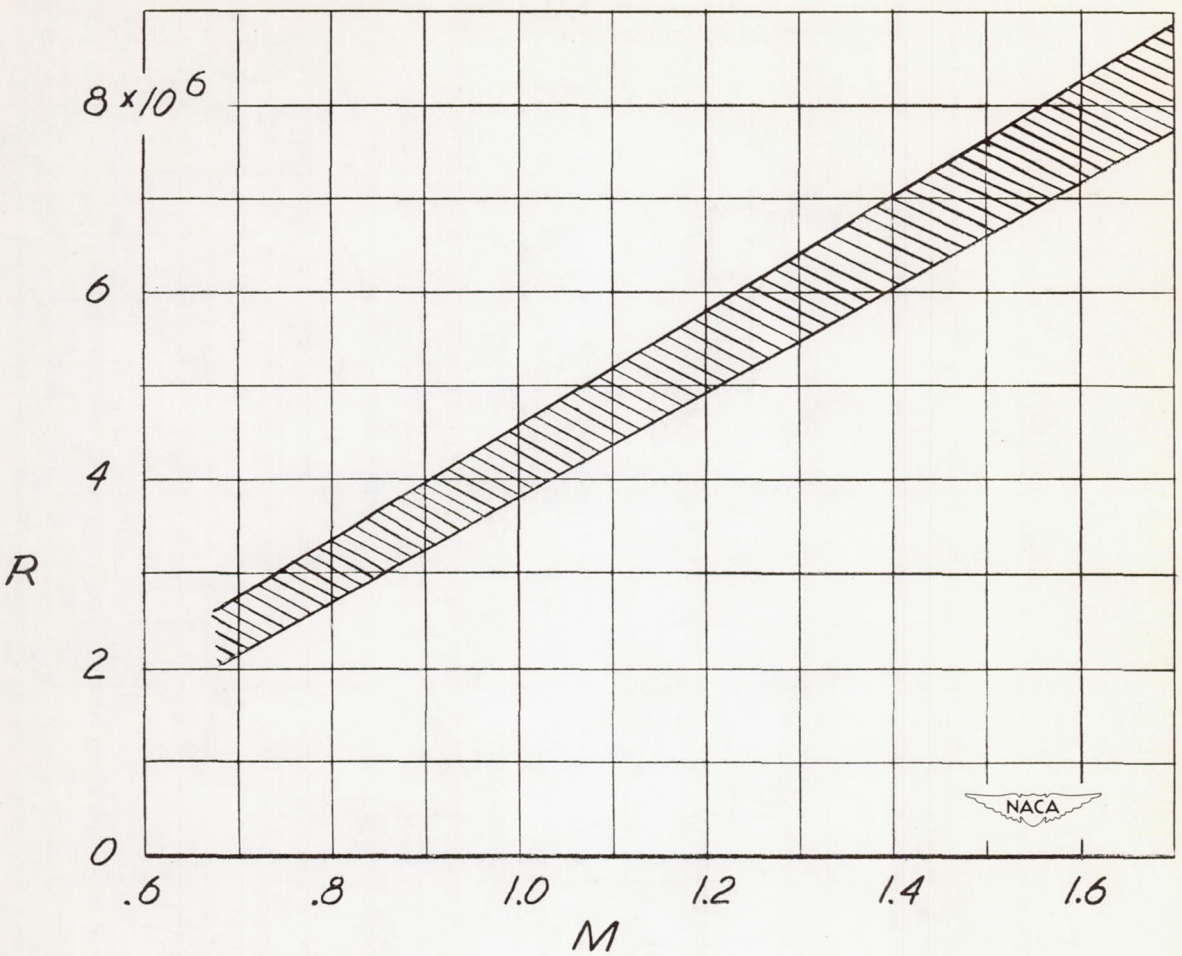

Figure 4.- Variation of test Reynolds number with Mach number. Reynolds number based on average wing chord, 0.72 foot.

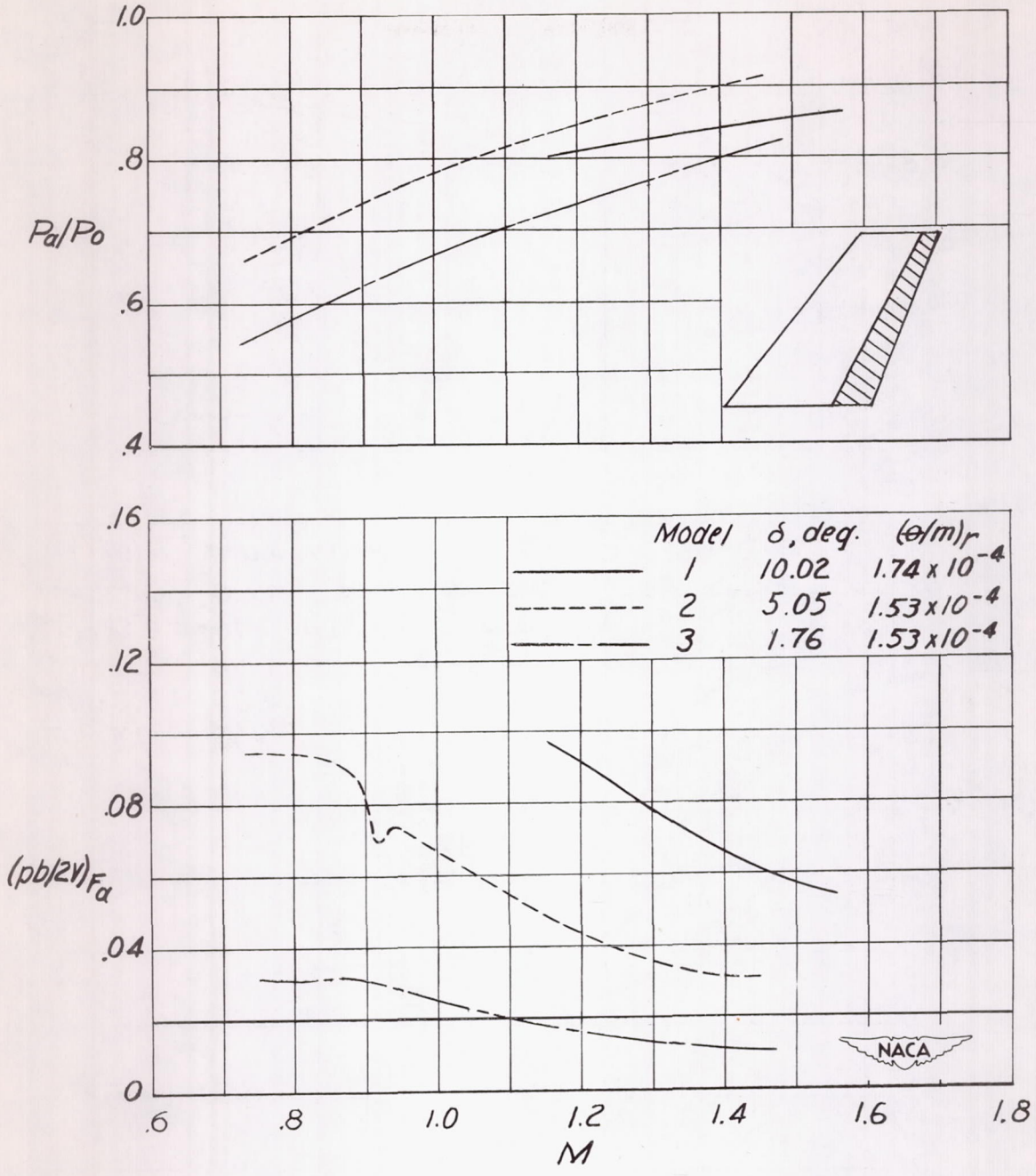

(a) $0.86\frac{b}{2}$ - span outboard ailerons; $\frac{c_a}{c} = 0.30$.

Figure 5.- Variation of P_a/P_o and rolling-effectiveness parameter $(pb/2V)_{F_a}$ with Mach number for ailerons on 35° sweptback wings; $(pb/2V)_{F_a}$ corrected to $i_w = 0$ but uncorrected for altitude.

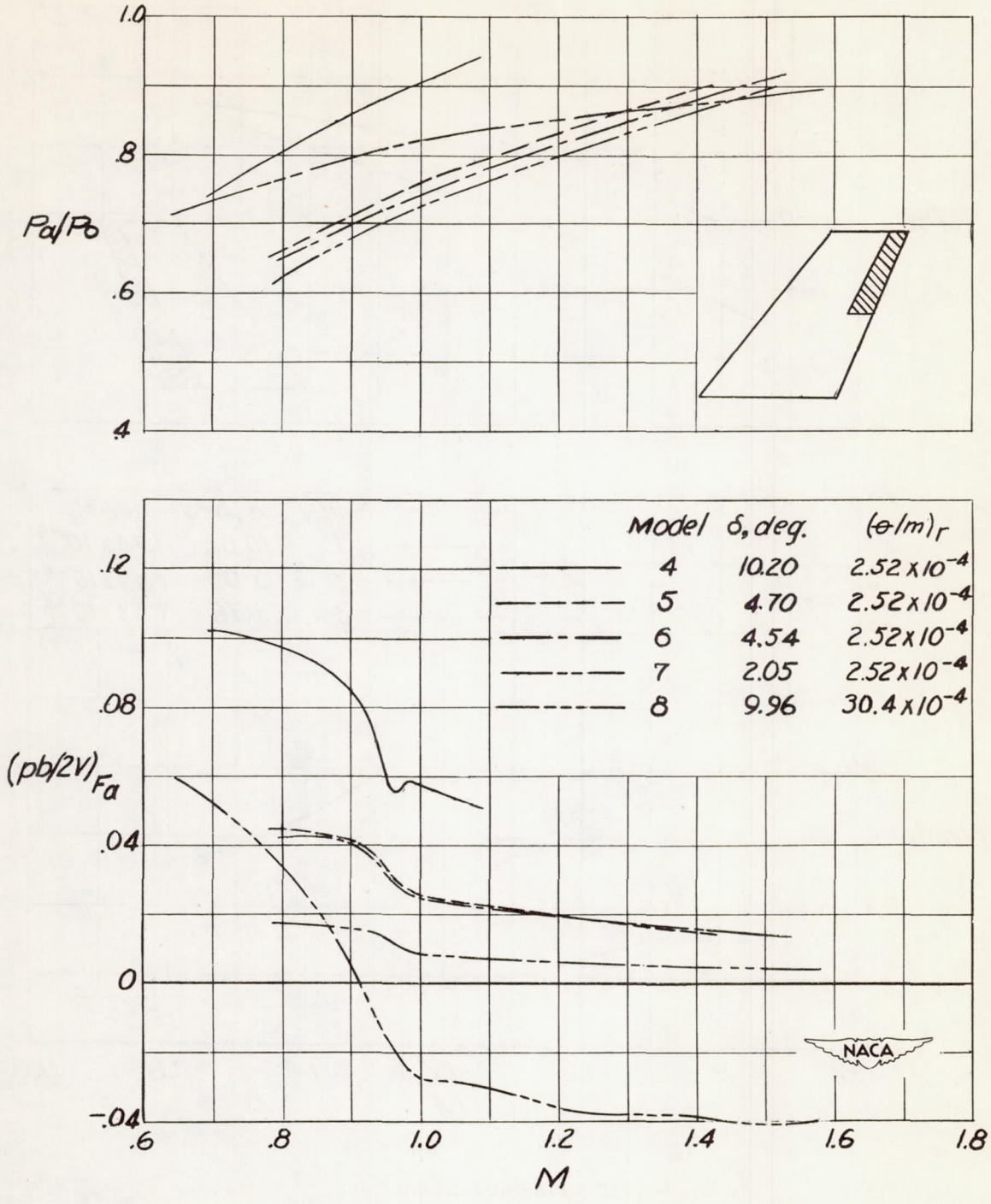

(b) $0.43\frac{b}{2}$ - span outboard ailerons; $\frac{c_a}{c} = 0.30$.

Figure 5.- Concluded.

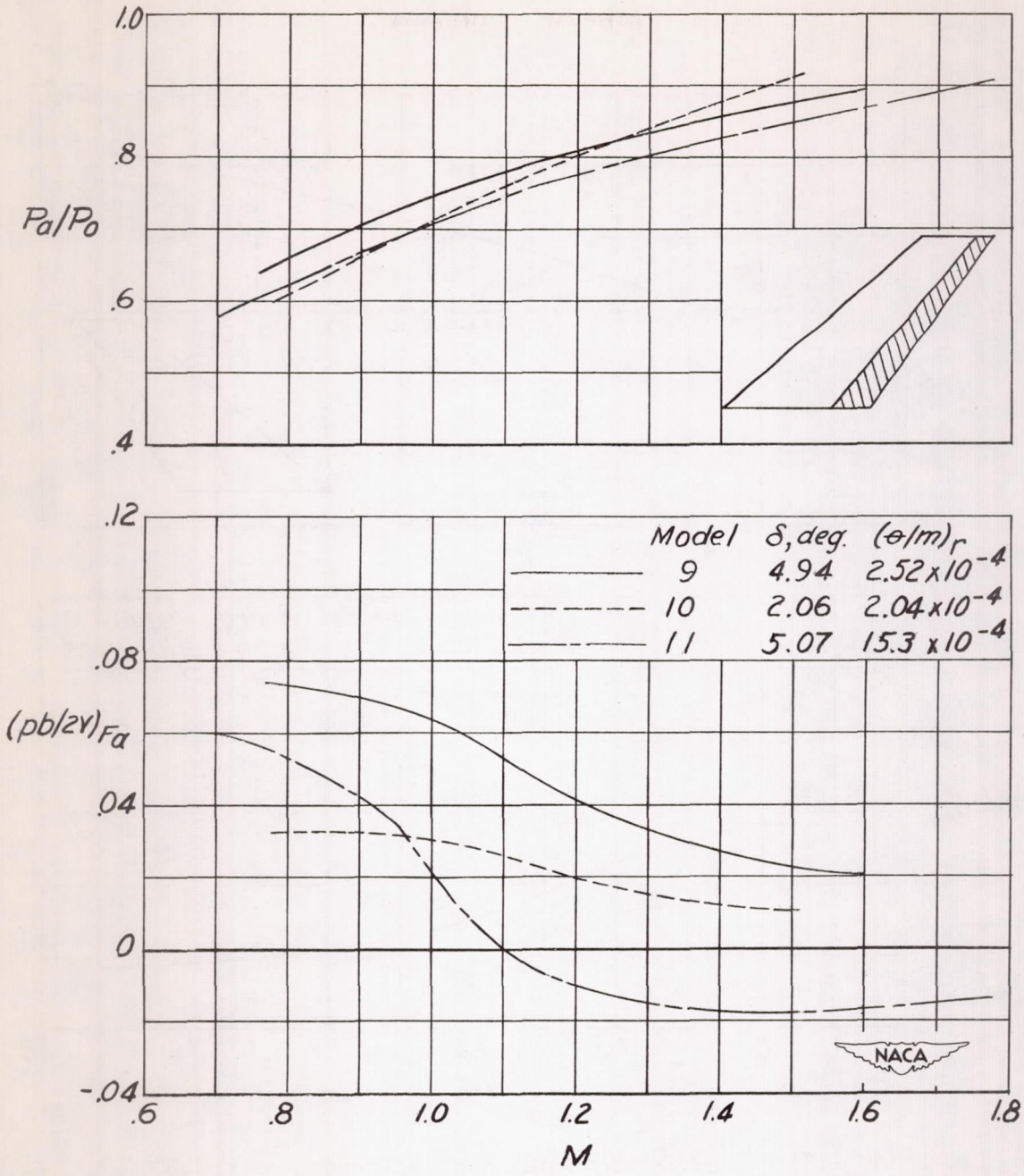

(a) $0.86\frac{b}{2}$ - span outboard aileron; $\frac{c_a}{c} = 0.30$.

Figure 6.- Variation of P_a/P_o and rolling-effectiveness parameter $(pb/2V)_{F_a}$ with Mach number for ailerons on 45° sweptback wings; $(pb/2V)_{F_a}$ corrected to $i_w = 0$ but uncorrected for altitude.

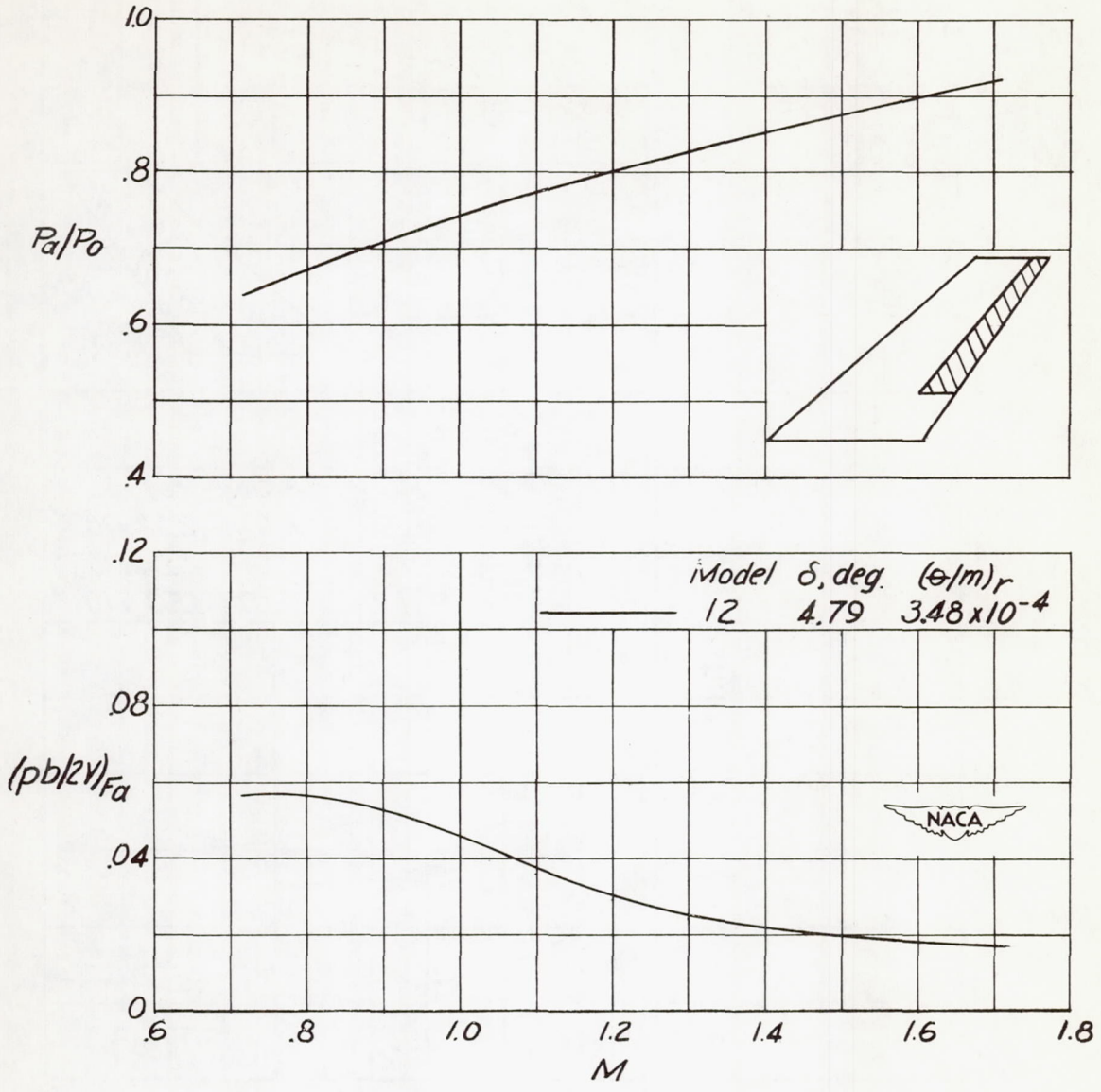

(b) $0.645\frac{b}{2}$ - span outboard aileron; $\frac{c_a}{c} = 0.30$.

Figure 6.- Continued.

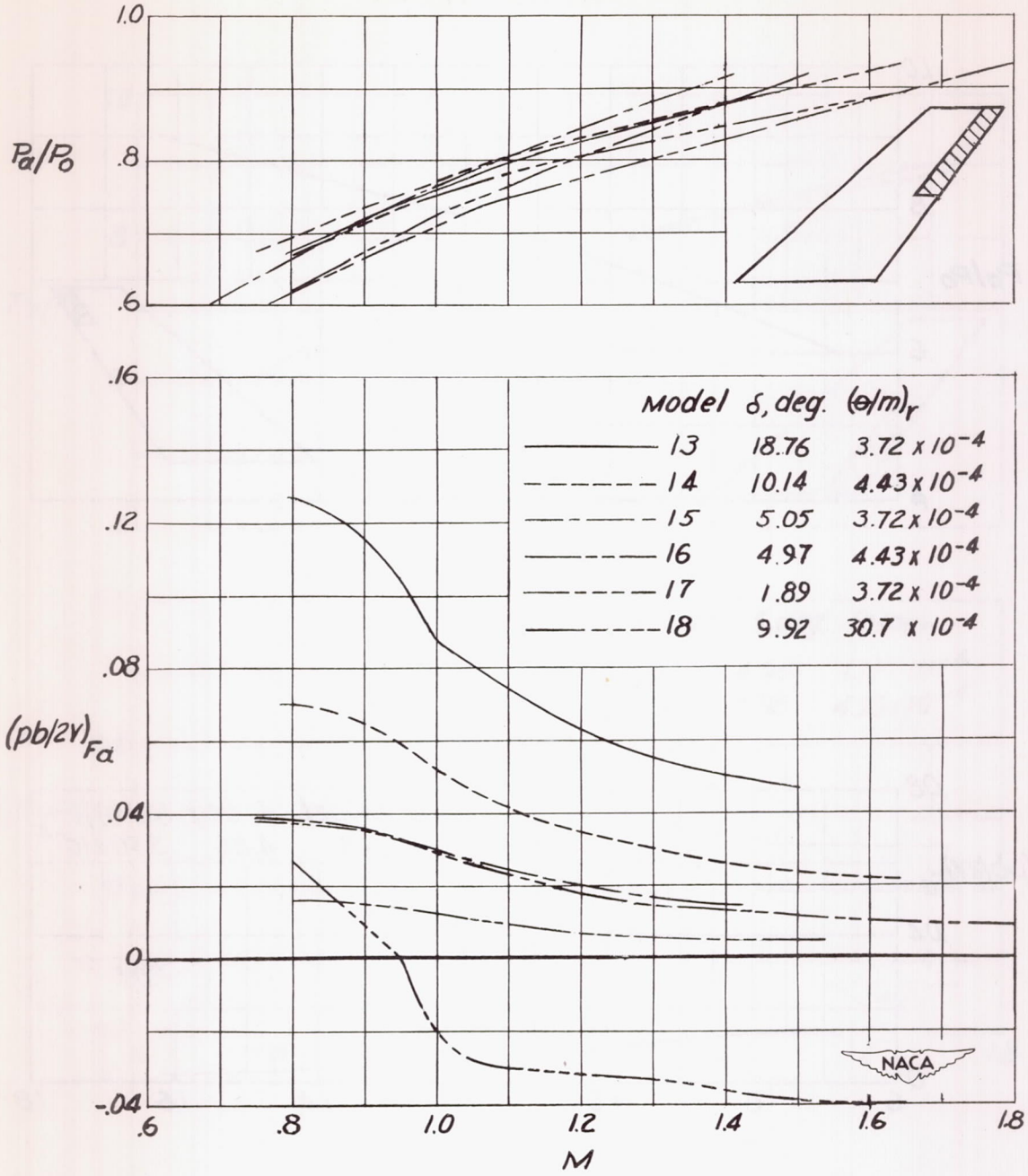

(c) $0.43\frac{b}{2}$ - span outboard aileron; $\frac{c_a}{c} = 0.30$.

Figure 6.- Continued.

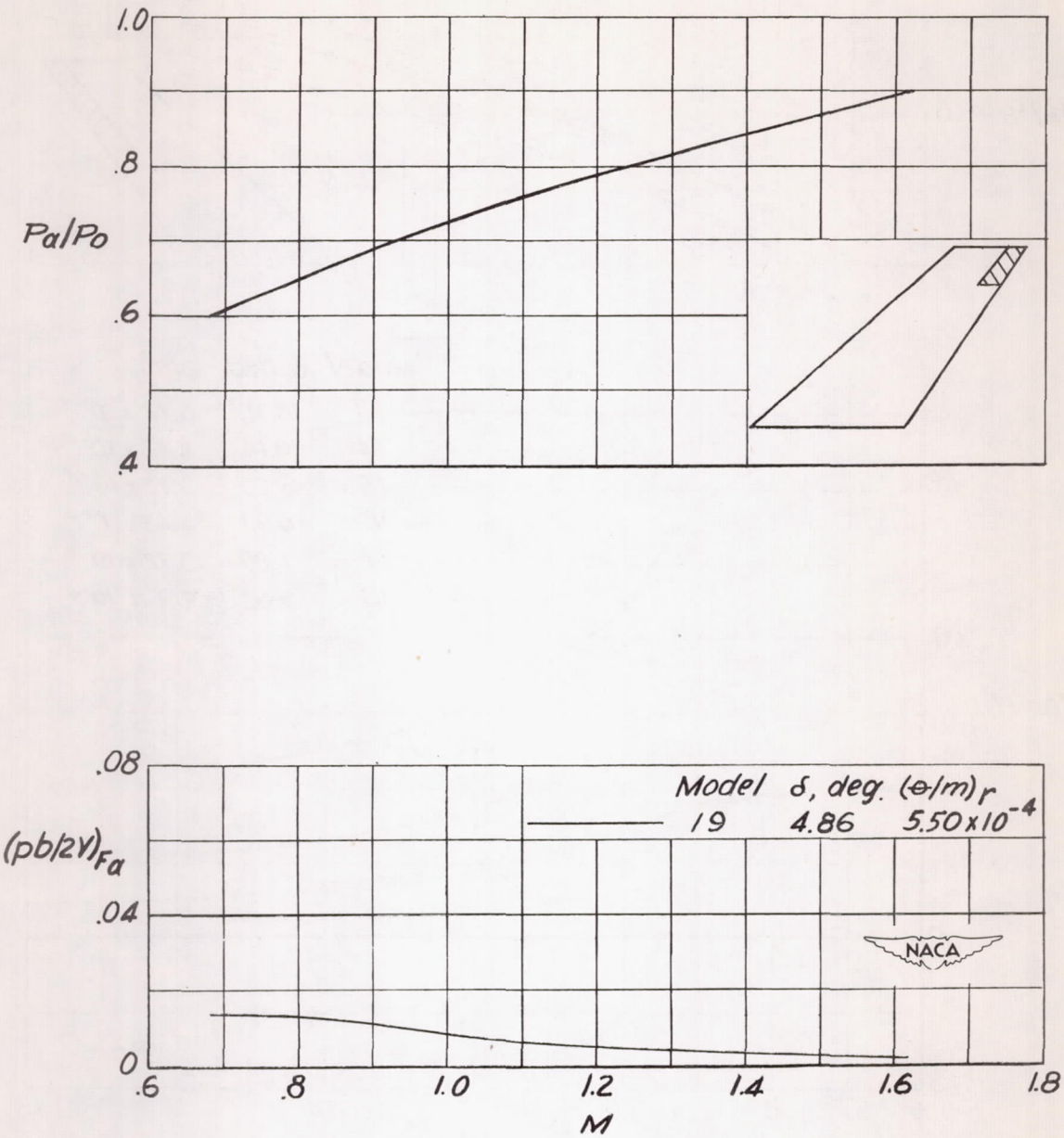

(d) $0.215\frac{b}{2}$ - span outboard aileron; $\frac{c_a}{c} = 0.30$.

Figure 6.- Continued.

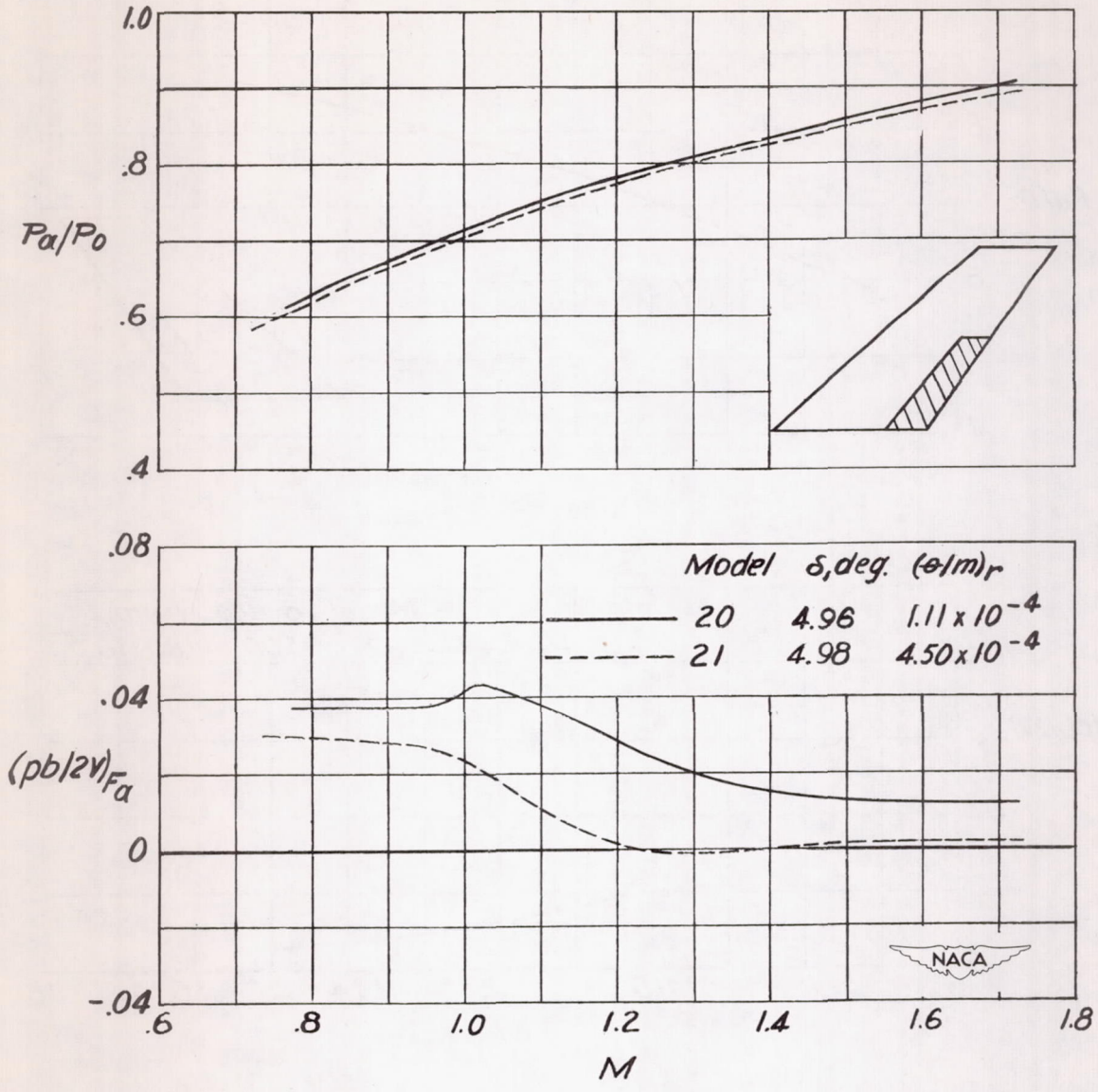

(e) $0.43\frac{b}{2}$ - span inboard aileron; $\frac{c_a}{c} = 0.30$.

Figure 6.- Continued.

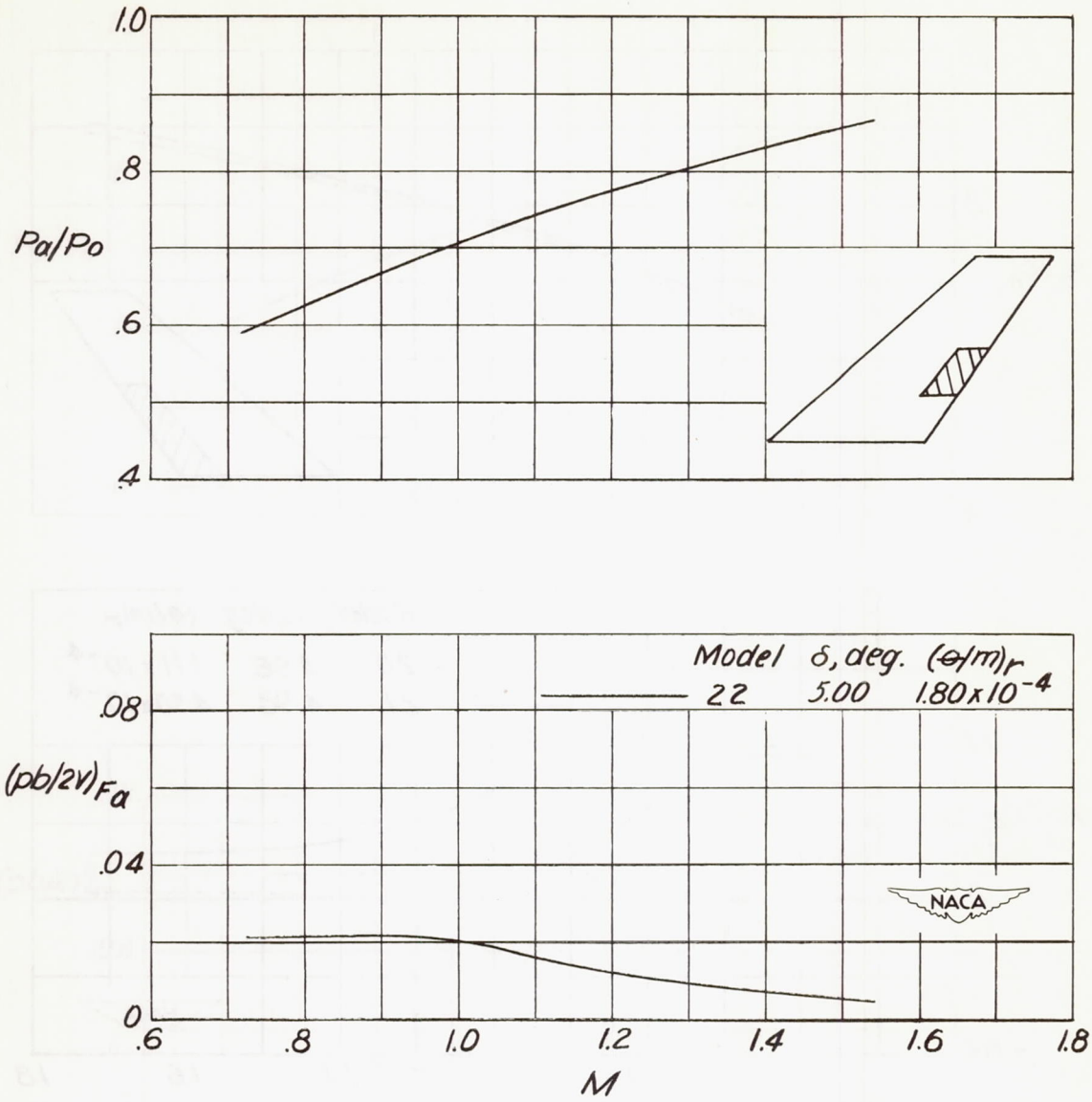

(f) $0.215\frac{b}{2}$ - span aileron; $\frac{y_o}{b/2} = 0.57$; $\frac{c_a}{c} = 0.30$.

Figure 6.- Continued.

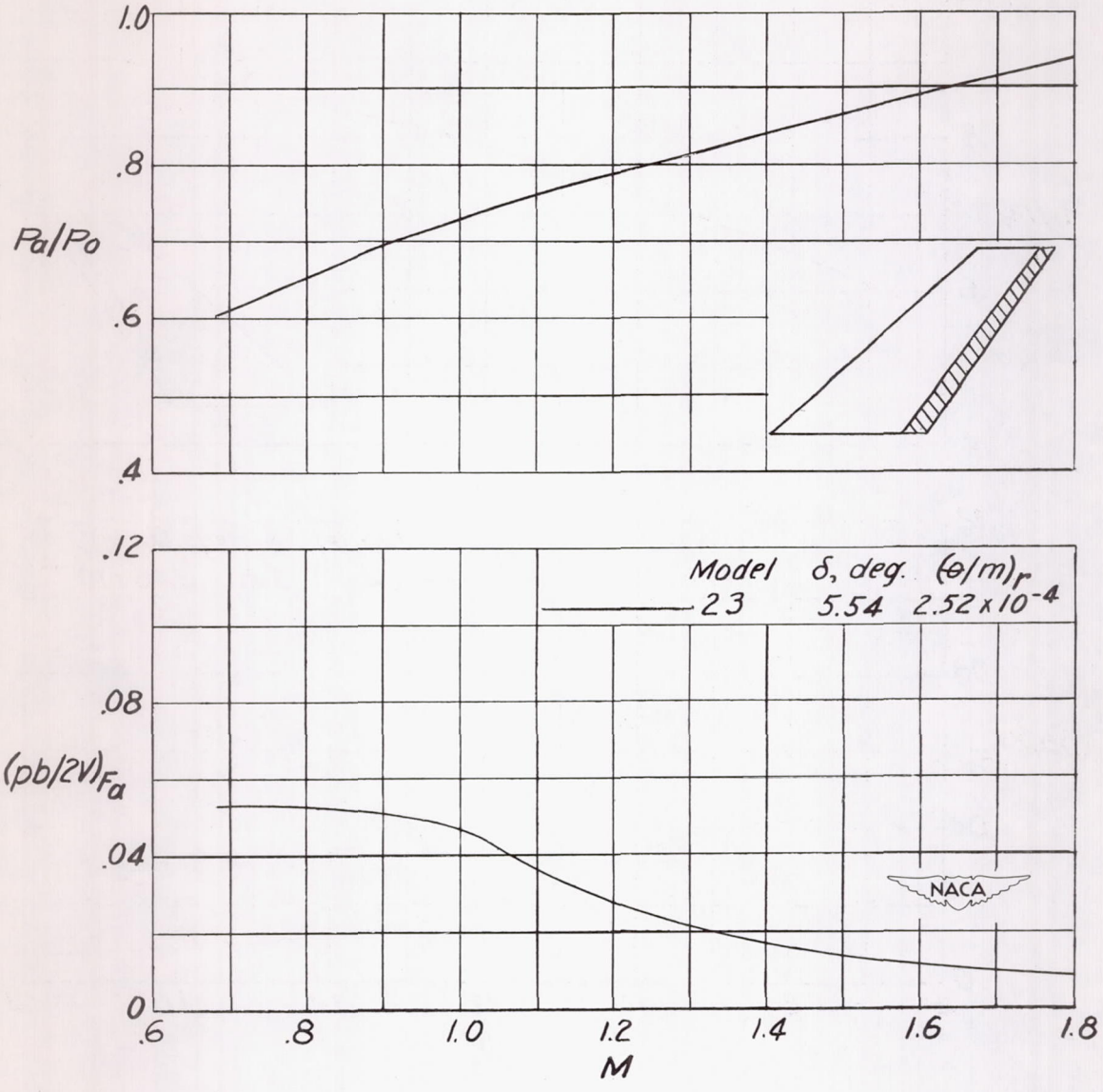

(g) $0.86\frac{b}{2}$ - span outboard aileron; $\frac{c_a}{c} = 0.15$.

Figure 6.- Continued.

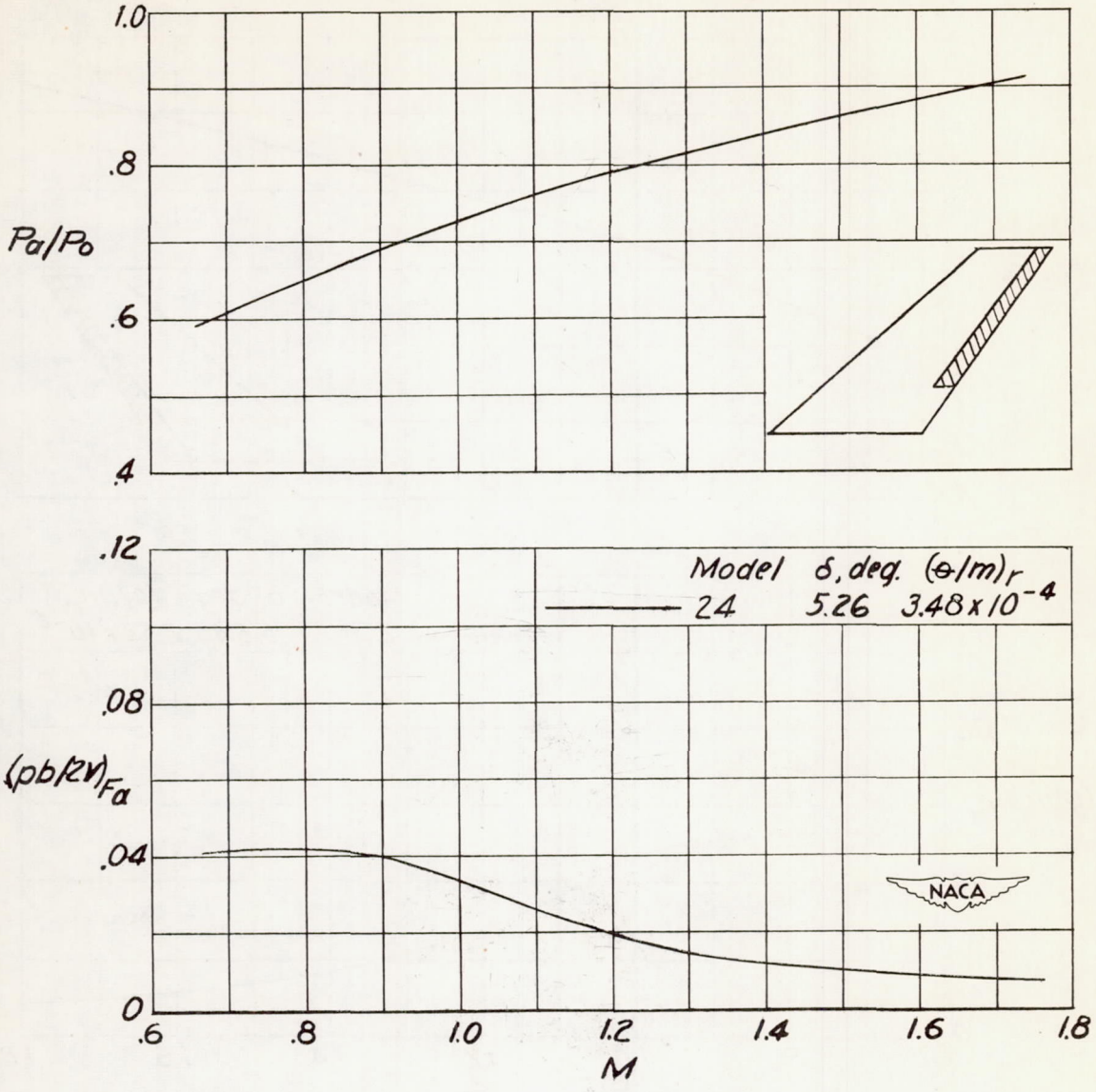

(h) $0.645\frac{b}{2}$ - span outboard aileron; $\frac{c_a}{c} = 0.15$.

Figure 6.- Continued.

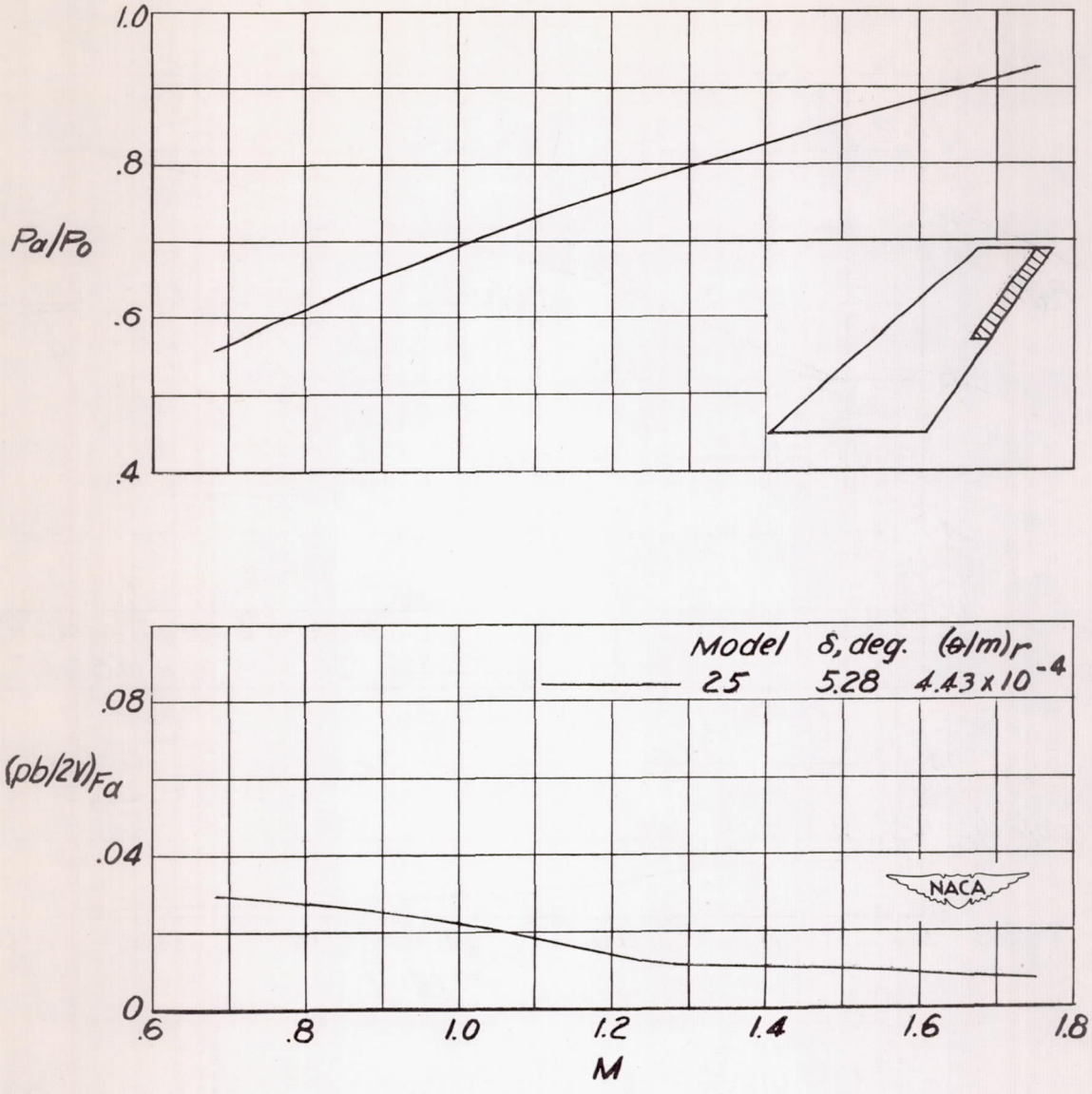

(i) $0.43\frac{b}{2}$ - span outboard aileron; $\frac{c_a}{c} = 0.15$.

Figure 6.- Continued.

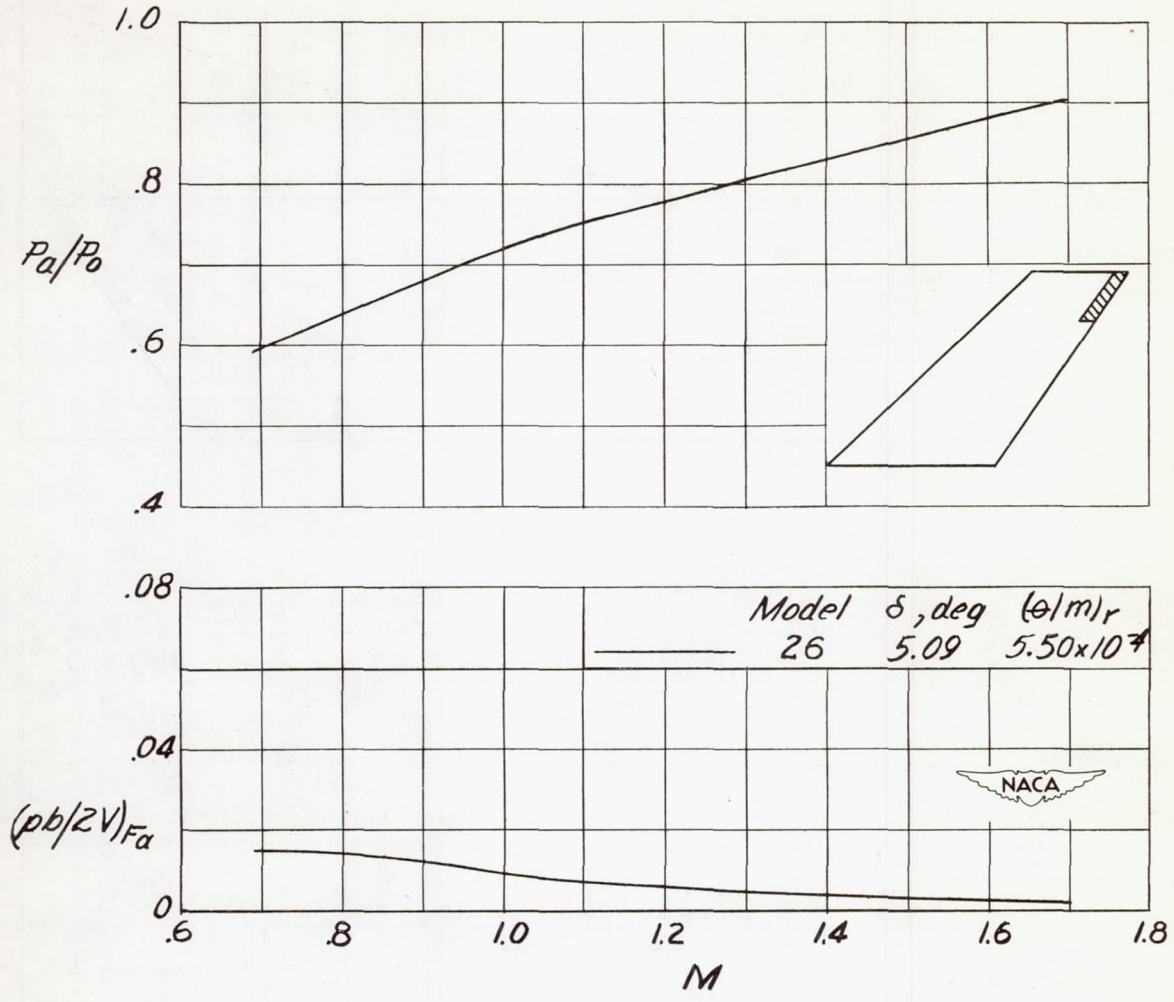

(j) $0.215\frac{b}{2}$ - span outboard aileron; $\frac{c_a}{c} = 0.15$.

Figure 6.- Continued.

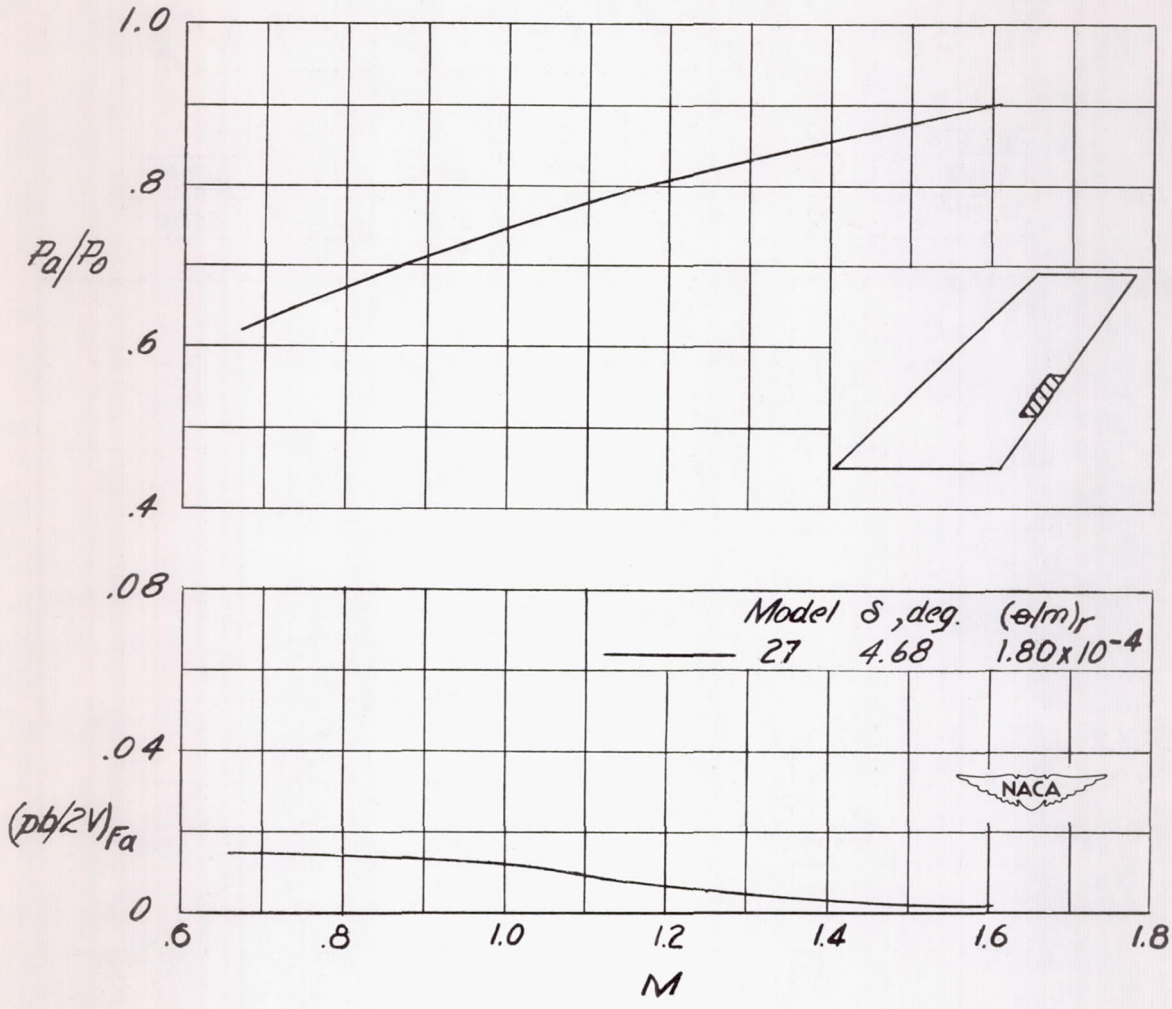

(k) $0.215\frac{b}{2}$ - span aileron; $\frac{y_o}{b/2} = 0.57$; $\frac{c_a}{c} = 0.15$.

Figure 6.- Concluded.

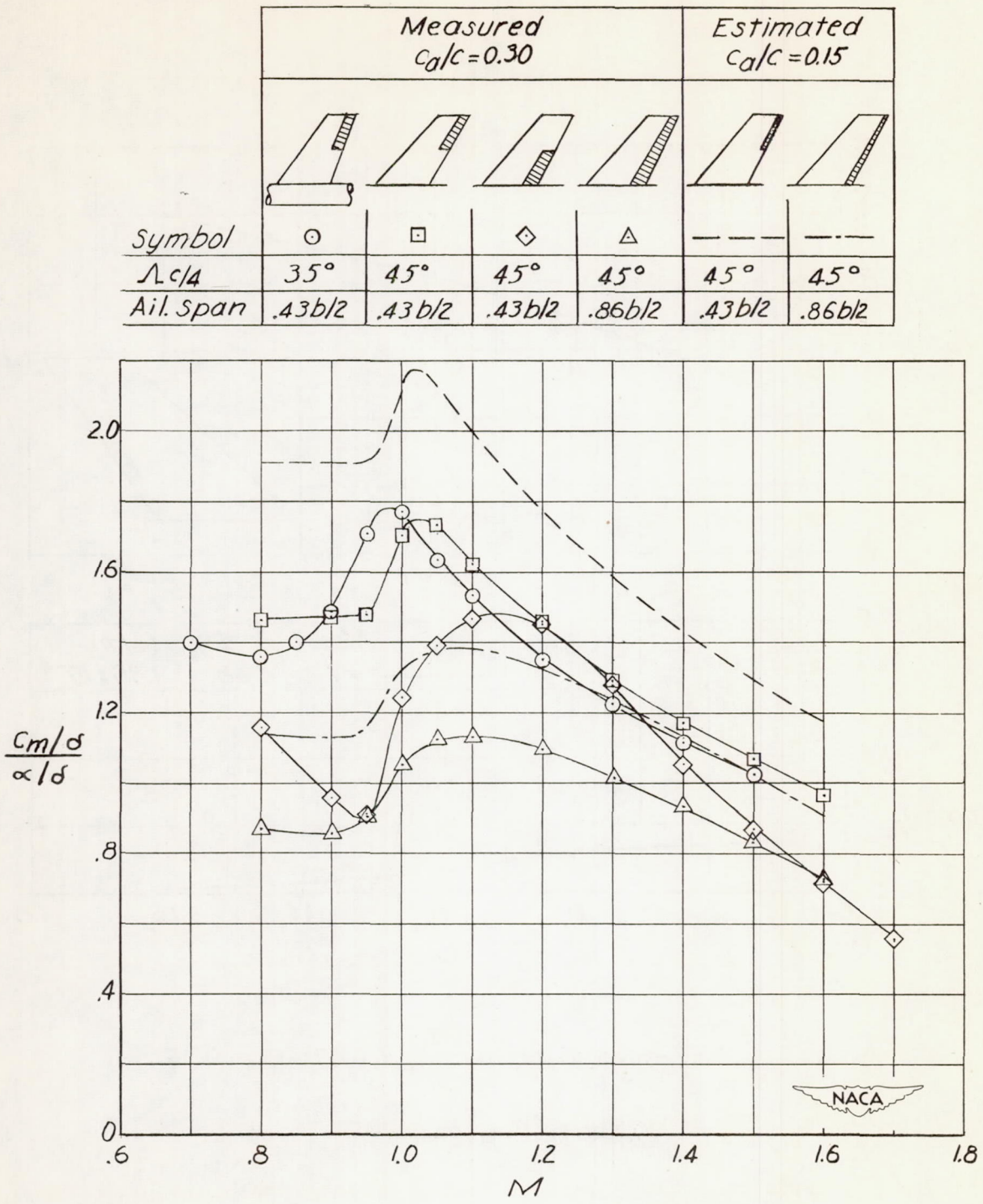

Figure 7.- Variation with Mach number of the effective twisting-moment coefficient evaluated from experimental flexible-wing rolling-effectiveness data.

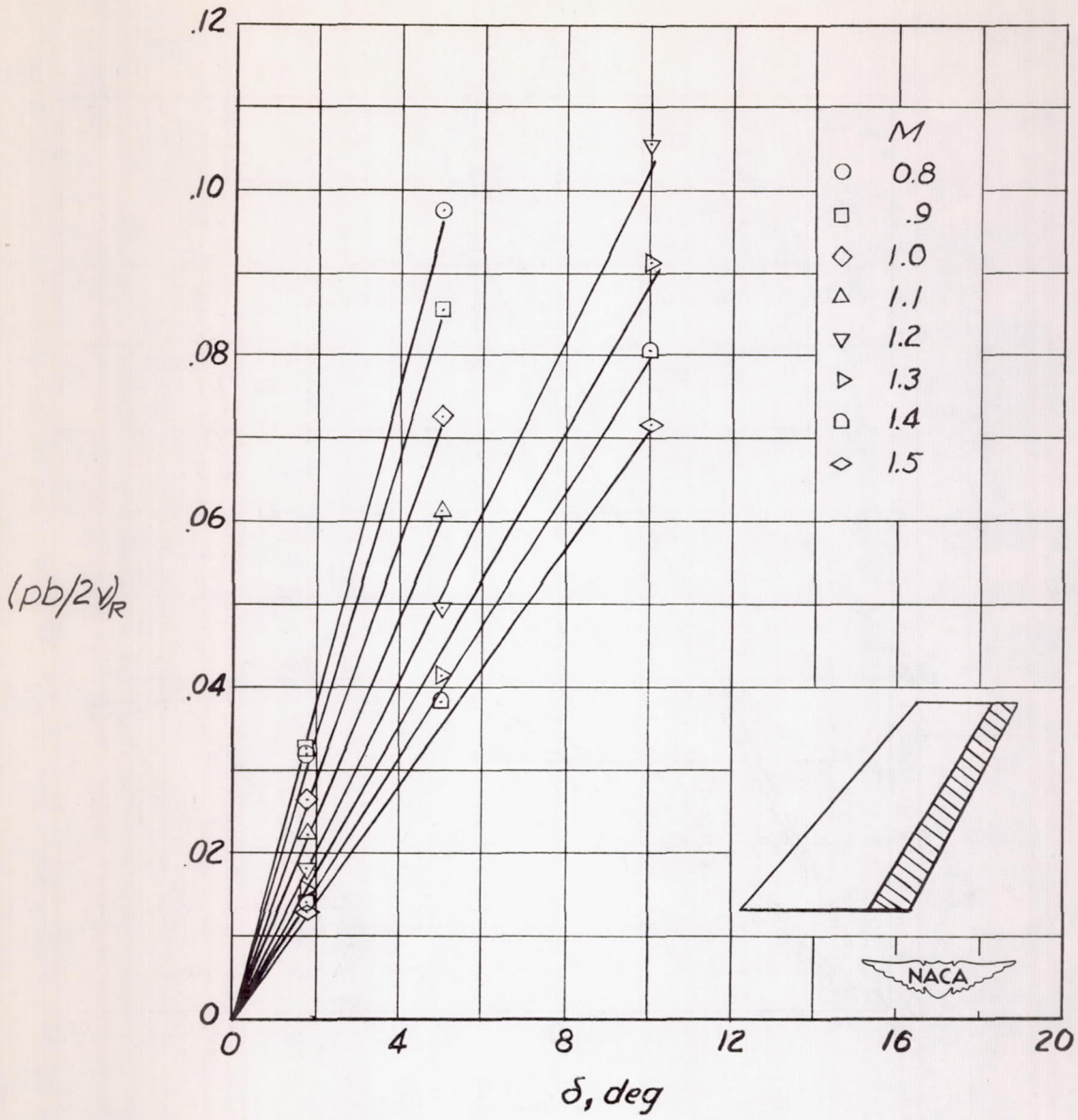

(a) $0.86\frac{b}{2}$ - span ailerons.

Figure 8.- Variation of rigid-wing rolling effectiveness with aileron deflection for outboard ailerons on 35° sweptback wings; $\frac{c_a}{c} = 0.30$.

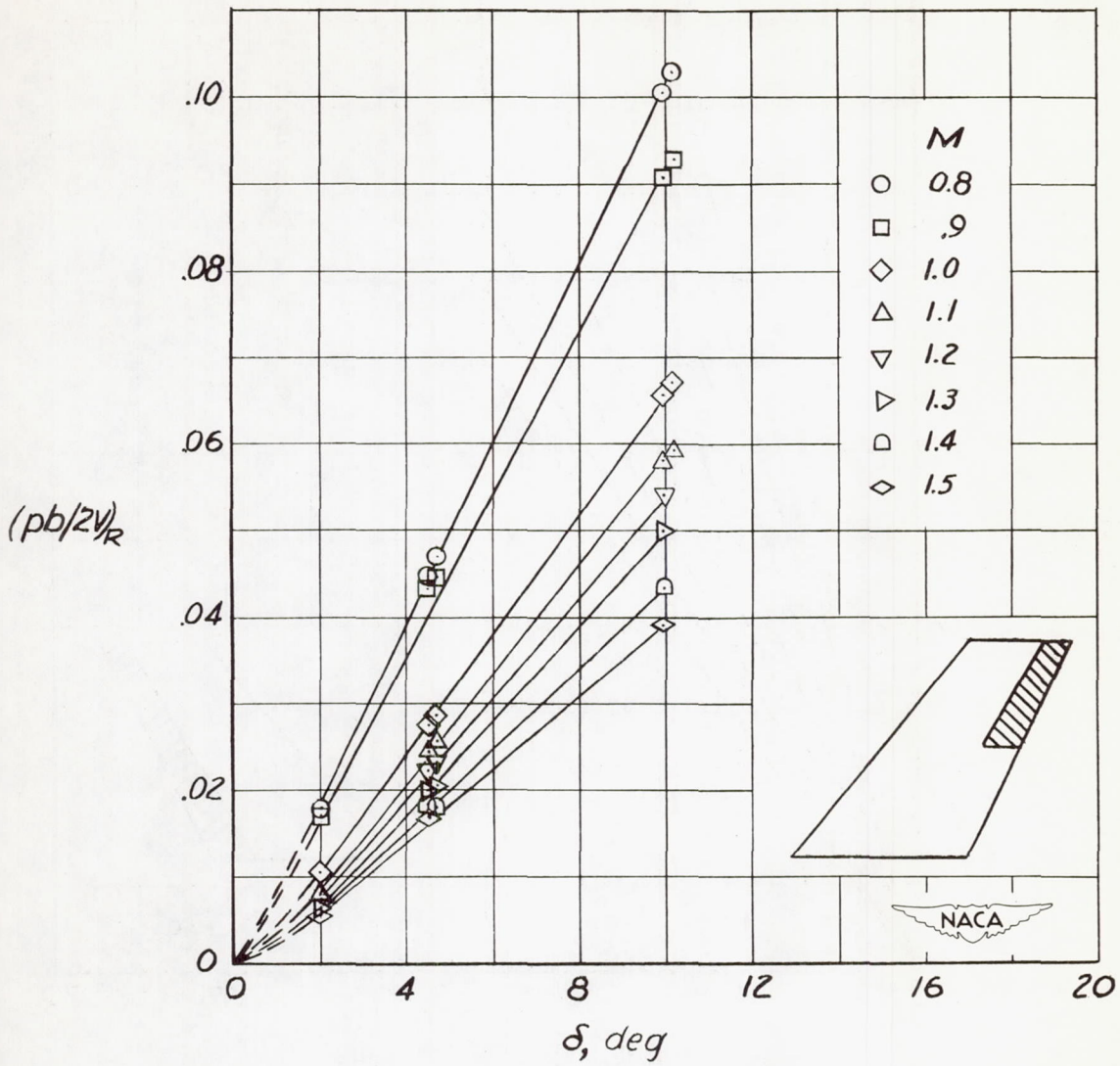

(b) $0.43\frac{b}{2}$ - span ailerons.

Figure 8.- Concluded.

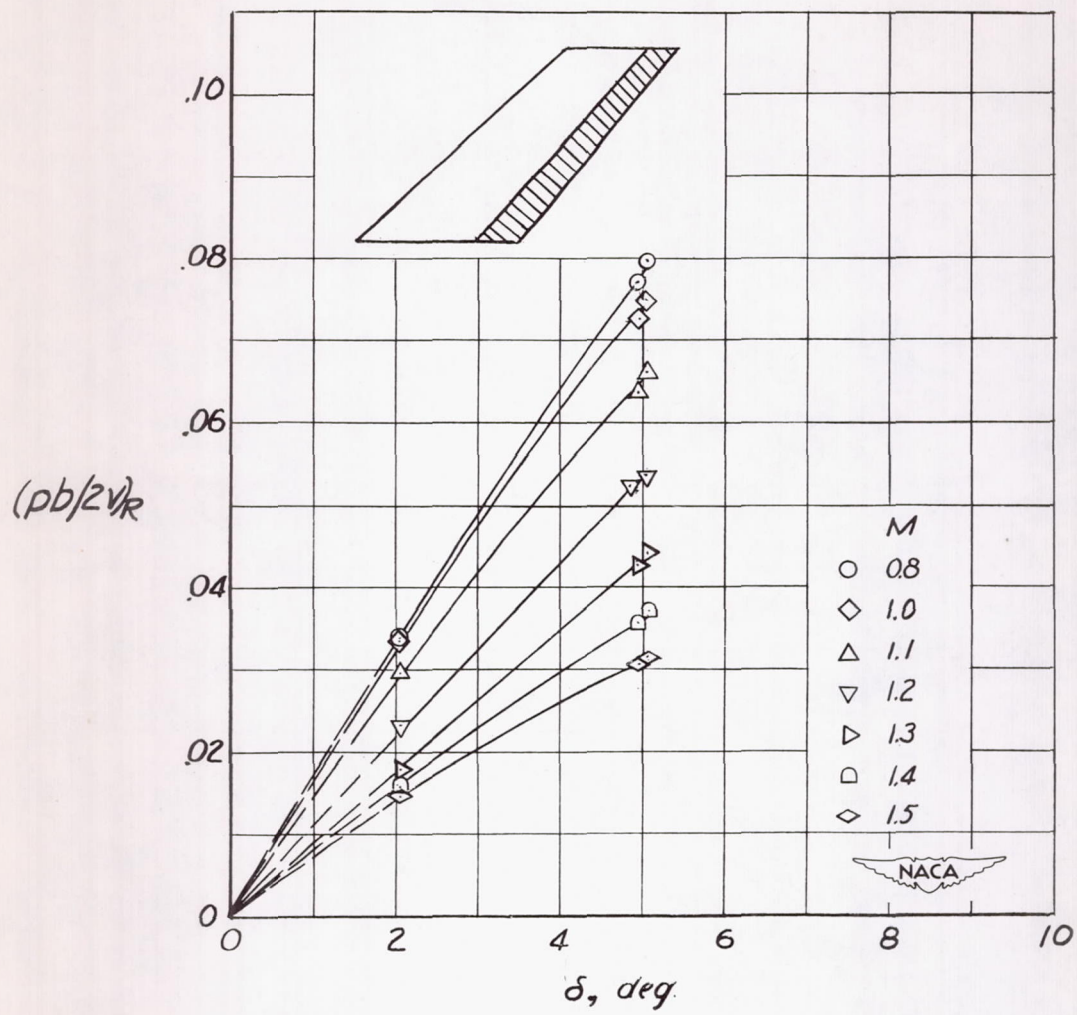

(a) $0.86\frac{b}{2}$ - span ailerons.

Figure 9.- Variation of rigid-wing rolling effectiveness with aileron deflection for outboard ailerons on 45° sweptback wings; $\frac{c_a}{c} = 0.30$.

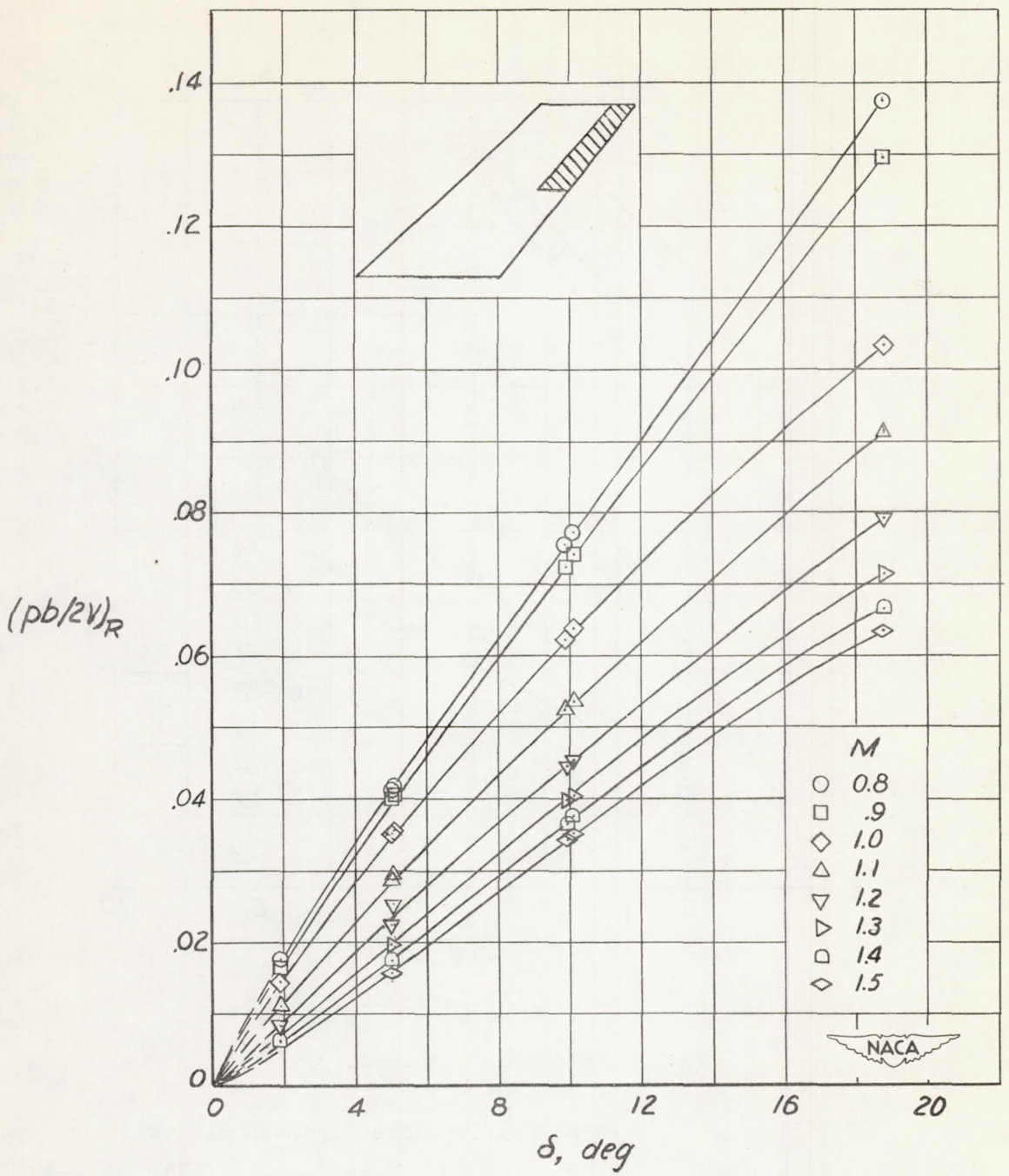

(b) $0.43\frac{b}{2}$ - span ailerons.

Figure 9.- Concluded.

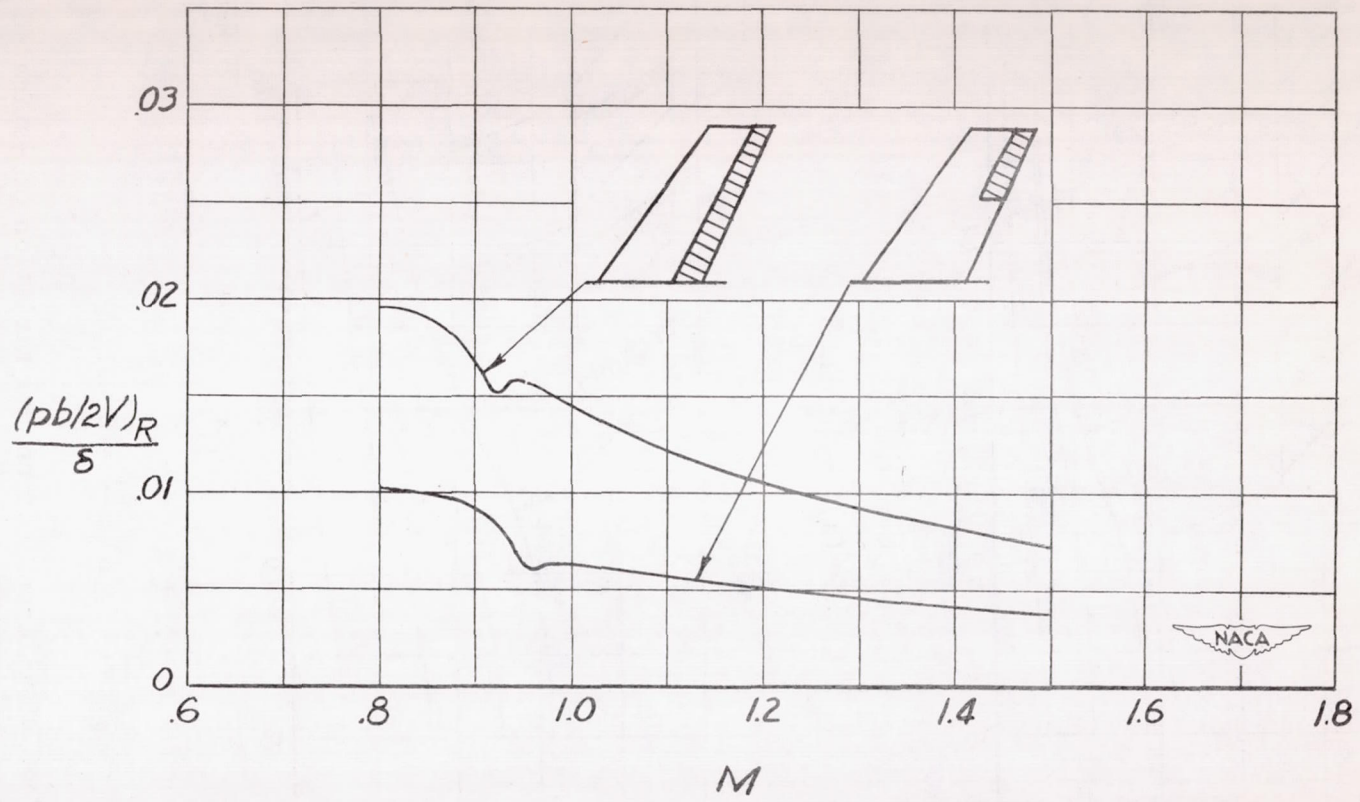

Figure 10.- Effect of aileron span on the variation of rigid-wing rolling effectiveness with Mach number for 35° sweptback wings having $0.86\frac{b}{2}$ - span and $0.43\frac{b}{2}$ - span outboard ailerons; $\frac{c_a}{c} = 0.30$.

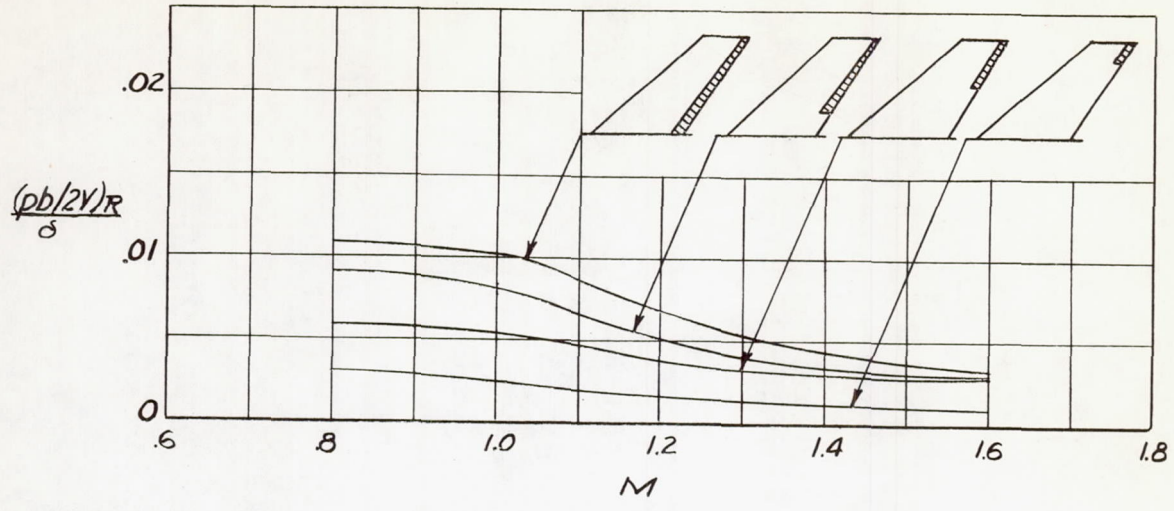

(a) $\frac{c_a}{c} = 0.15$.

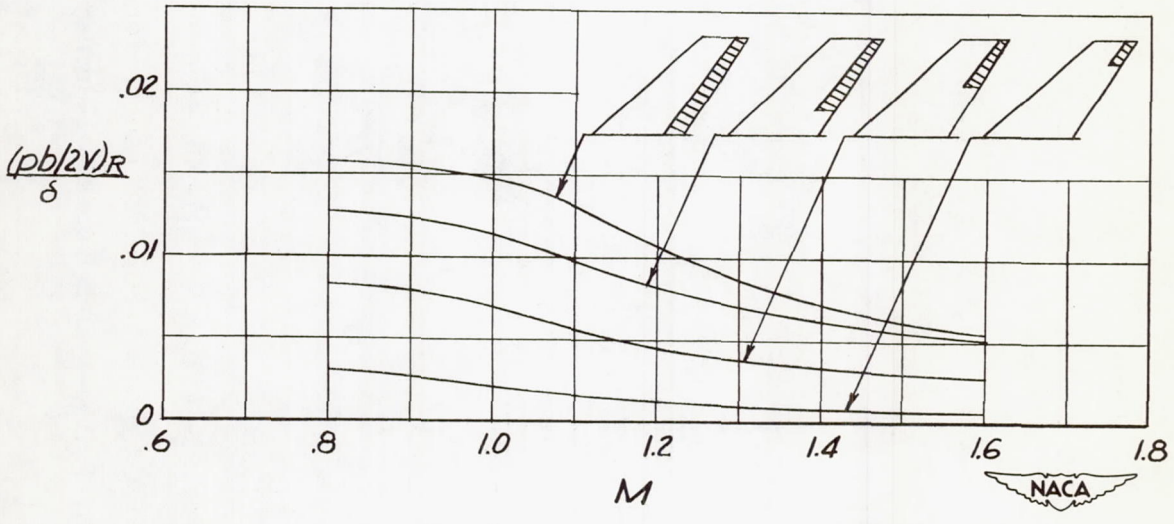

(b) $\frac{c_a}{c} = 0.30$.

Figure 11.- Effect of aileron span on the variation of estimated rigid-wing rolling effectiveness with Mach number for 45° sweptback wings having $0.86\frac{b}{2}$ - span, $0.645\frac{b}{2}$ - span, $0.43\frac{b}{2}$ - span, and $0.215\frac{b}{2}$ - span outboard ailerons.

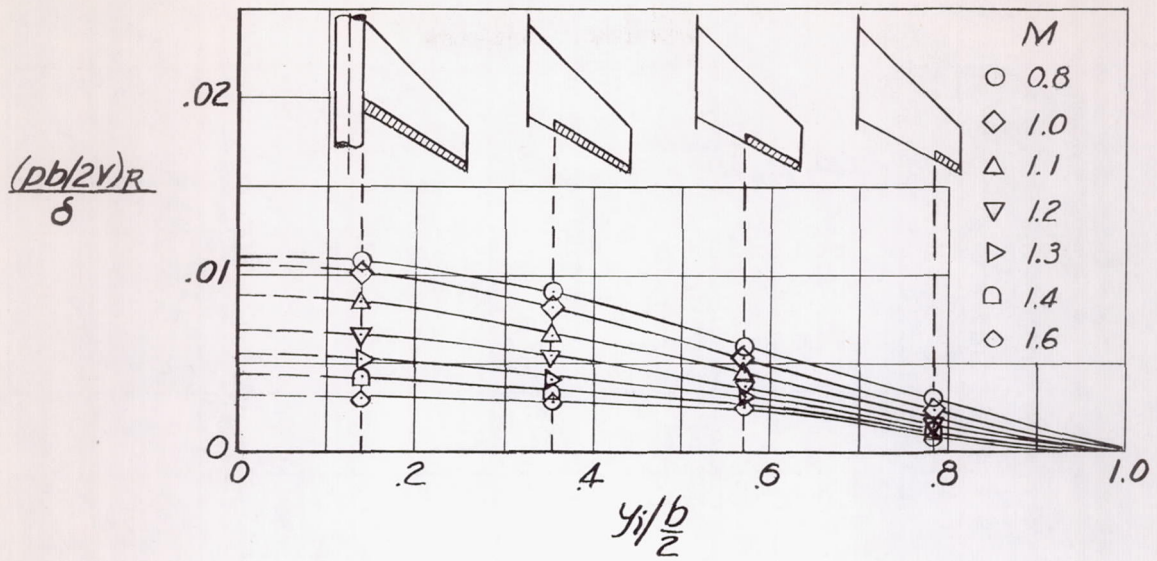

(a) $\frac{c_a}{c} = 0.15$.

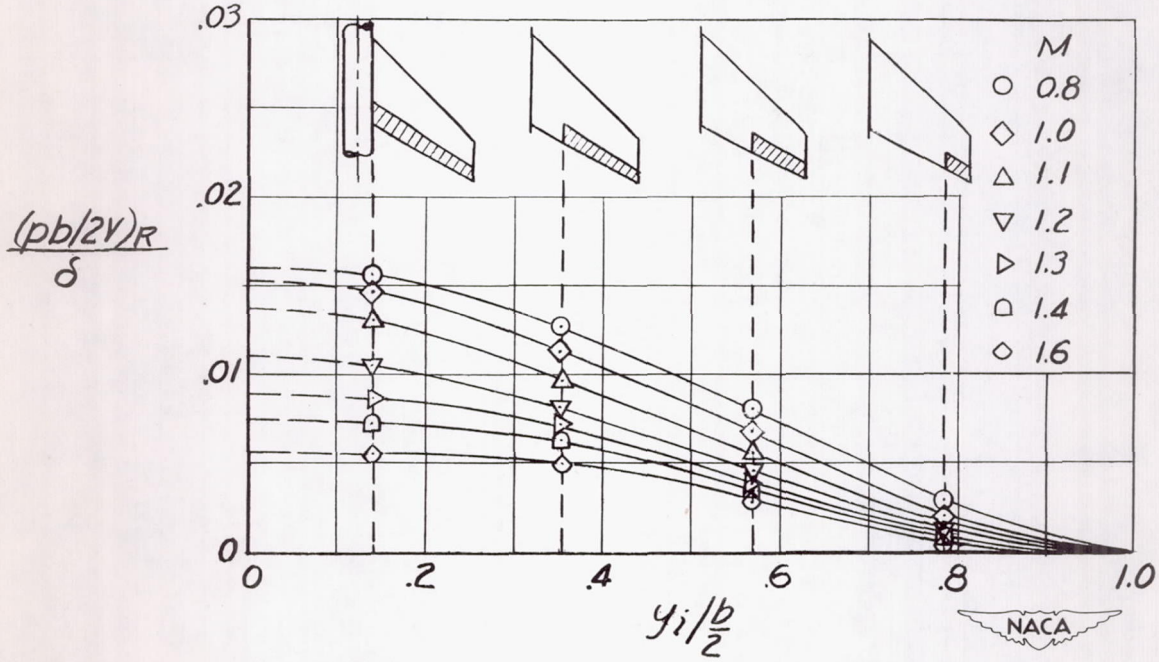

(b) $\frac{c_a}{c} = 0.30$.

Figure 12.- Variation of estimated rigid-wing rolling effectiveness with inboard extent of aileron span; $\Lambda = 45^{\circ}$.

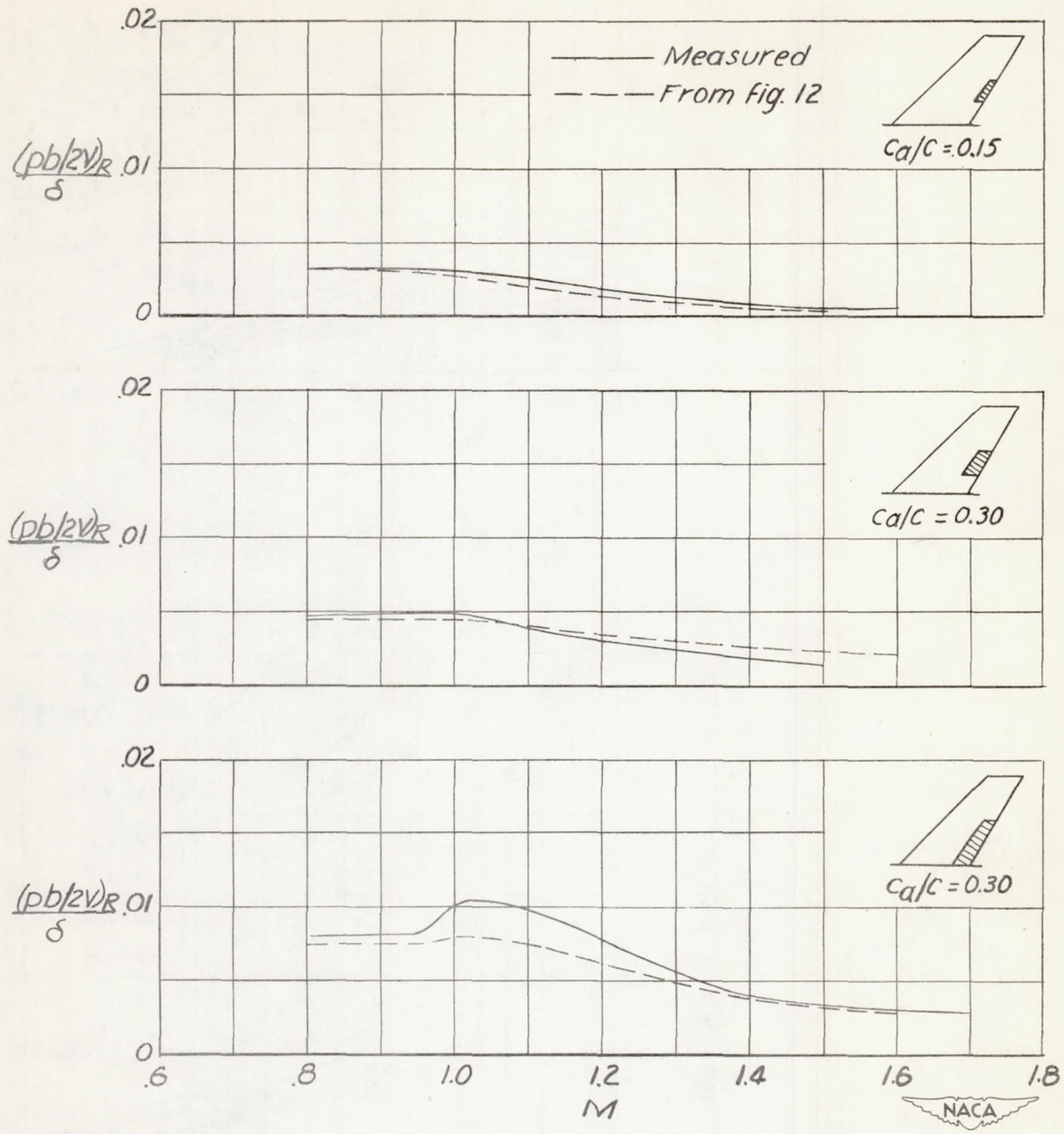

Figure 13.- Comparison of measured unit-aileron rolling-effectiveness data with values estimated from figure 12 for the $0.43\frac{b}{2}$-span inboard aileron and $0.215\frac{b}{2}$-span centrally located ailerons on 45° sweptback wings.

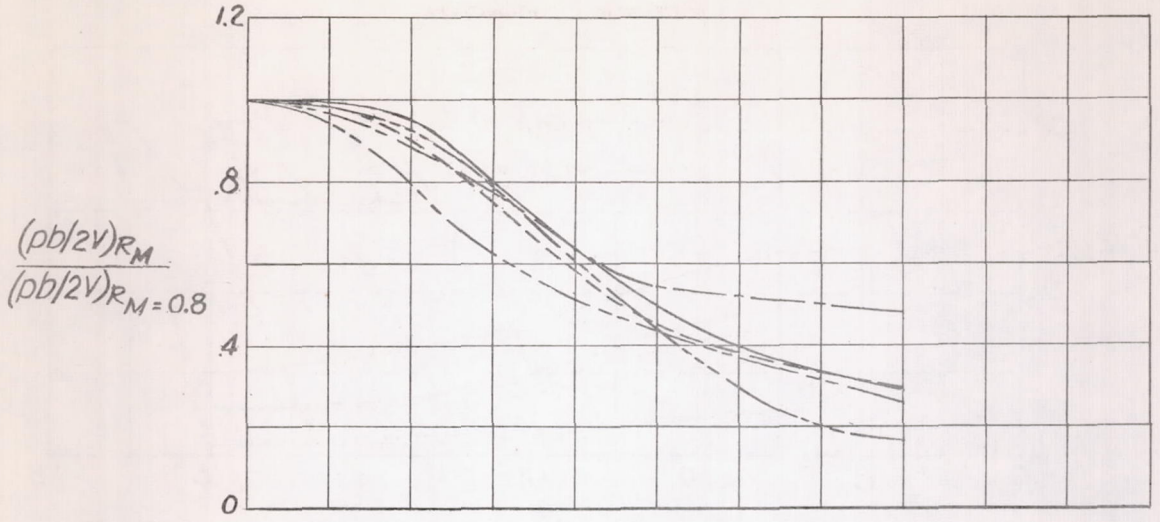

(a) $\frac{c_a}{c} = 0.15$.

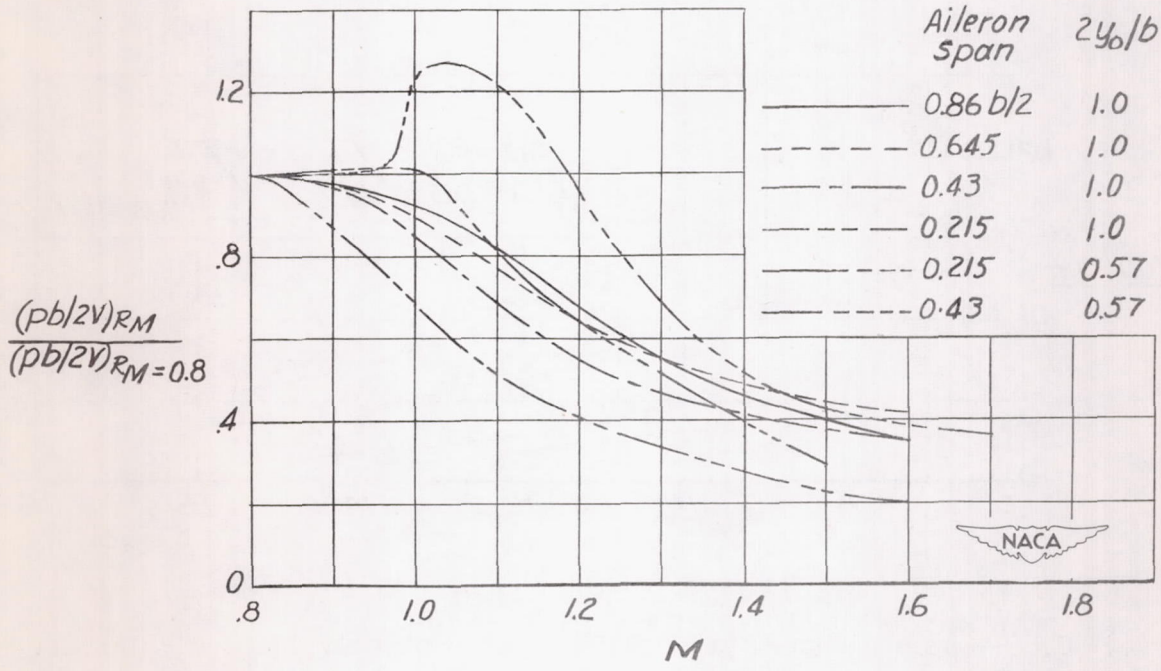

(b) $\frac{c_a}{c} = 0.30$.

Figure 14.- Fraction of rolling effectiveness at Mach number 0.8 retained over Mach number range for ailerons on 45° sweptback wings.

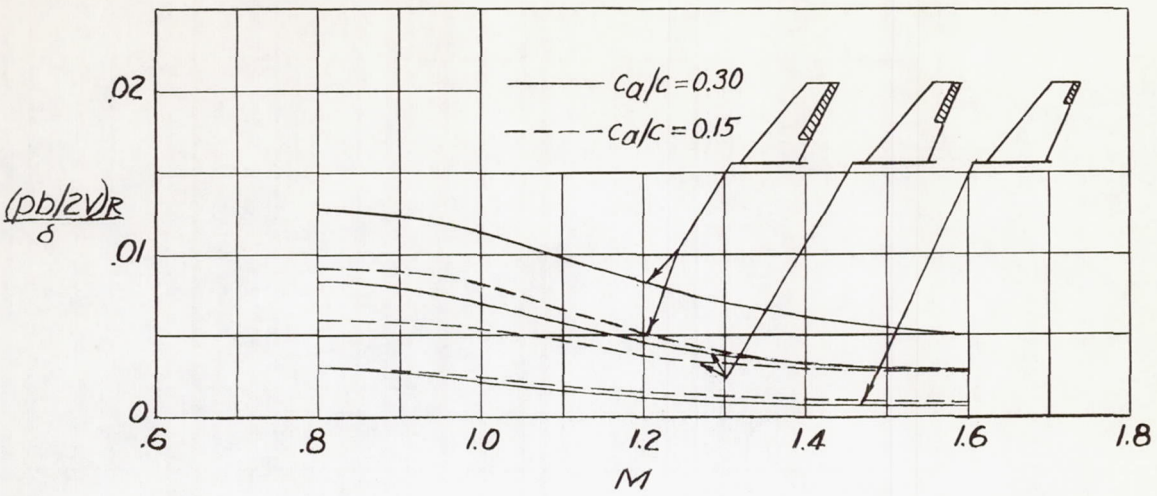

(a) $0.645\frac{b}{2}$ - span, $0.43\frac{b}{2}$ - span, and $0.215\frac{b}{2}$ - span ailerons.

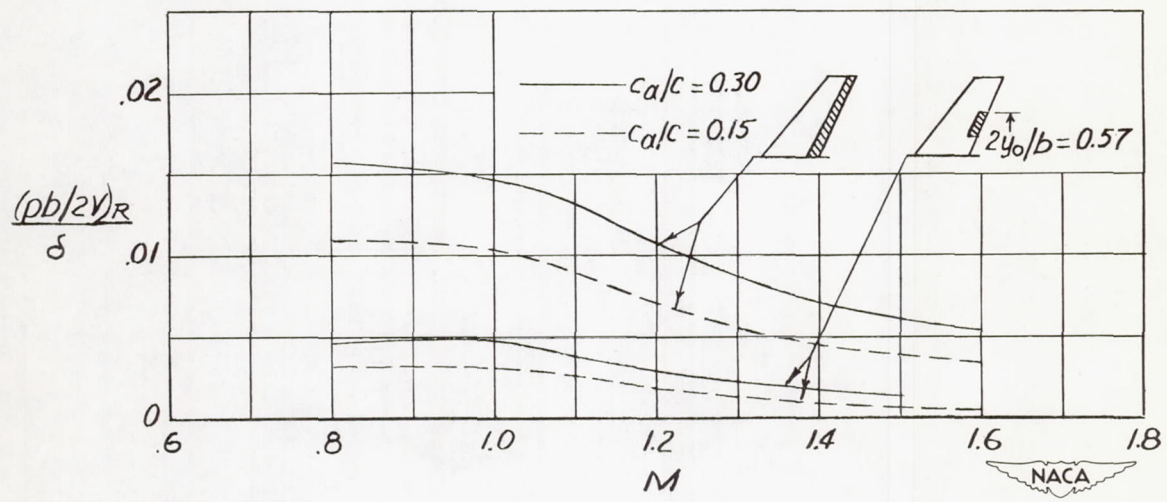

(b) $0.86\frac{b}{2}$ - span outboard and $0.215\frac{b}{2}$ - span centrally located ailerons.

Figure 15.- Effect of changing aileron-chord ratio on the variation of rolling effectiveness with Mach number for 45° sweptback wings.

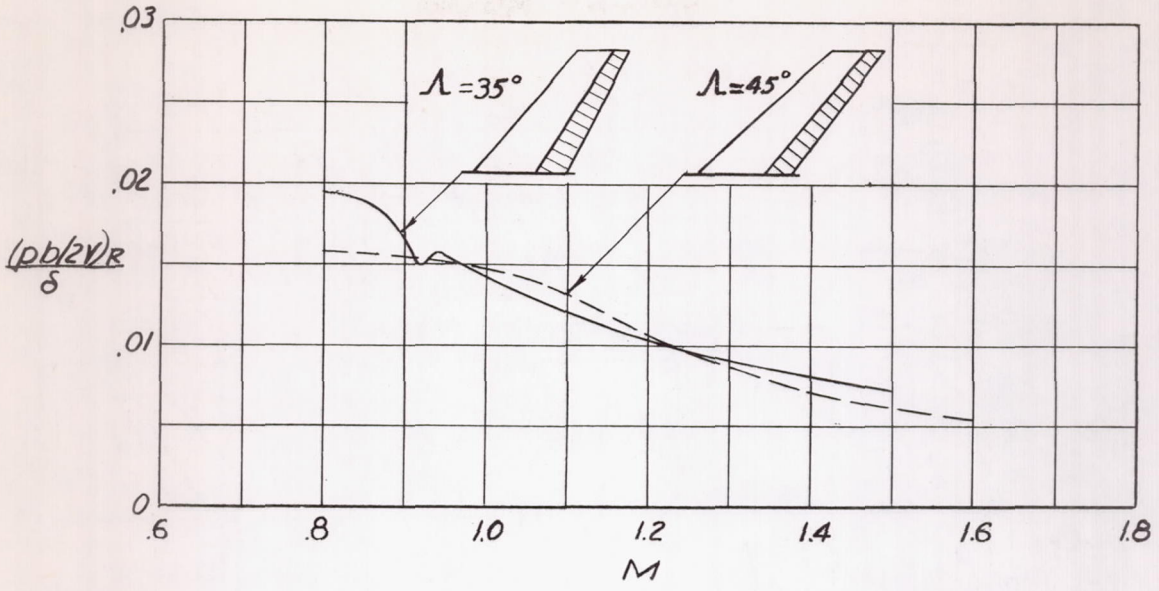

(a) $0.86\frac{b}{2}$ - span ailerons.

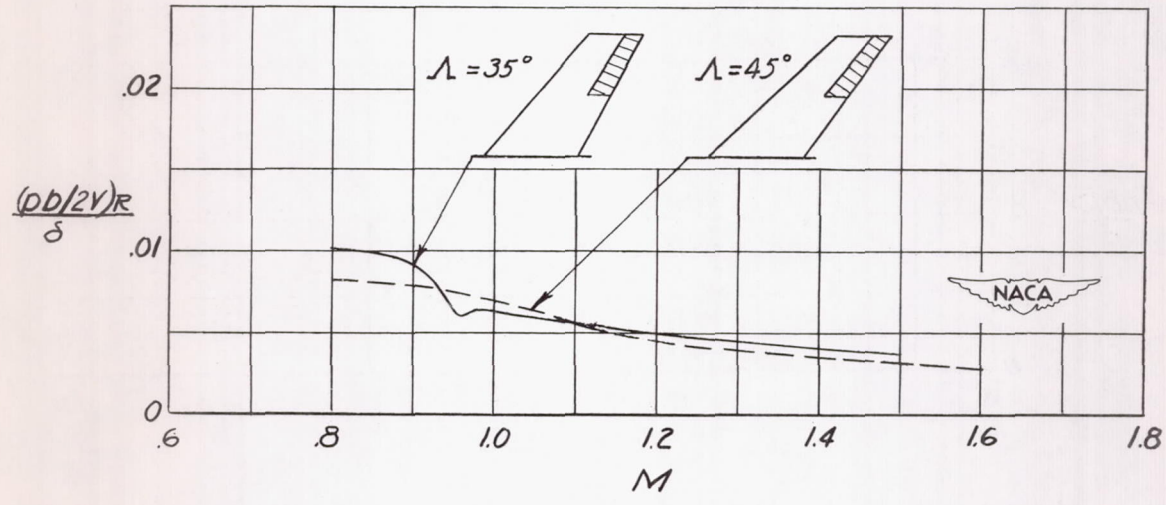

(b) $0.43\frac{b}{2}$ - span ailerons.

Figure 16.- Effect of sweepback on the variation of rolling effectiveness with Mach number for $0.86\frac{b}{2}$ - span and $0.43\frac{b}{2}$ - span outboard ailerons; $\frac{c_a}{c} = 0.30$.

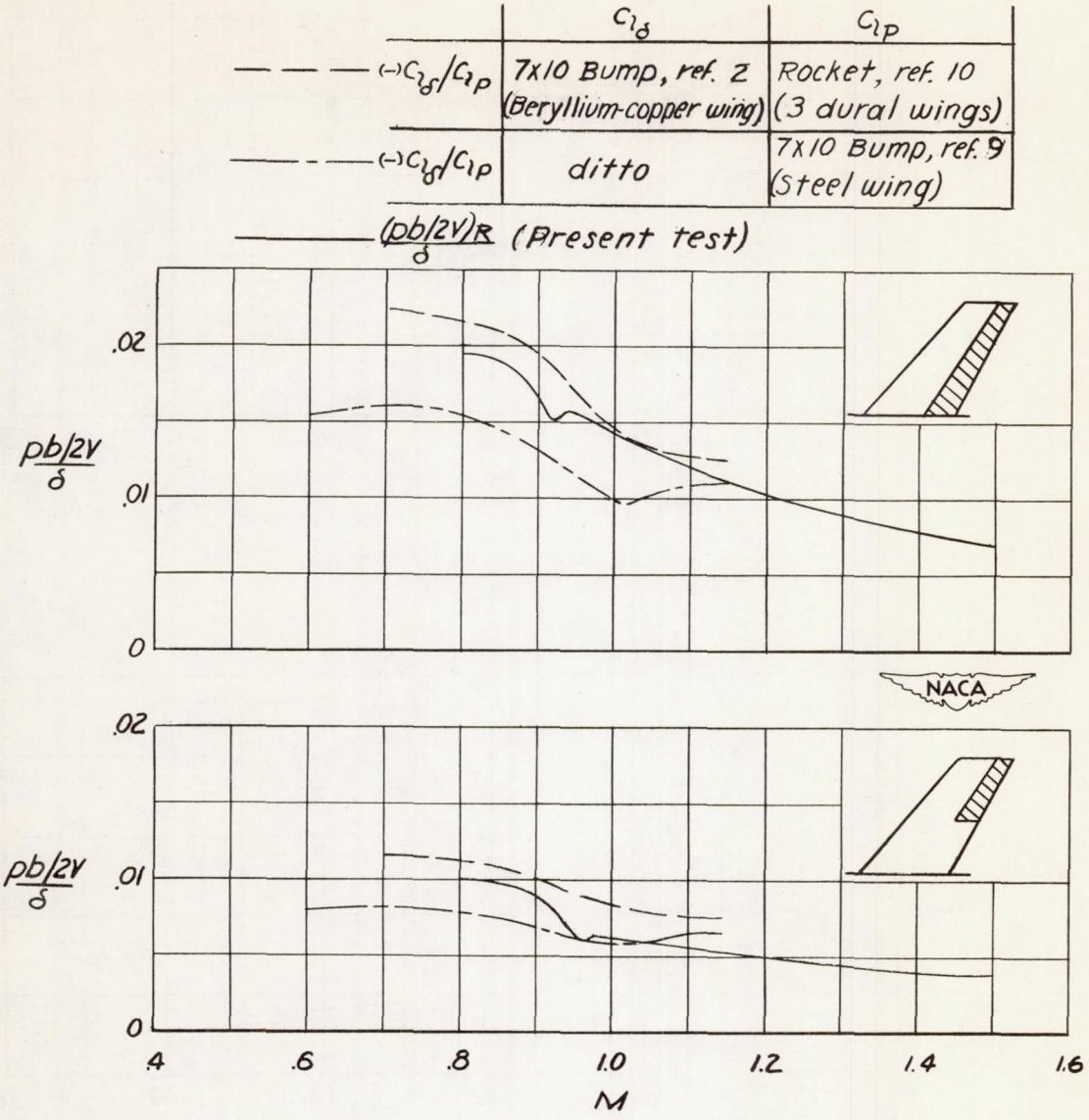

(a) 35° sweptback wings with $0.86\frac{b}{2}$ - span and $0.43\frac{b}{2}$ - span outboard ailerons.

Figure 17.- Comparison of test results with reference data; $\frac{c_a}{c} = 0.30$.

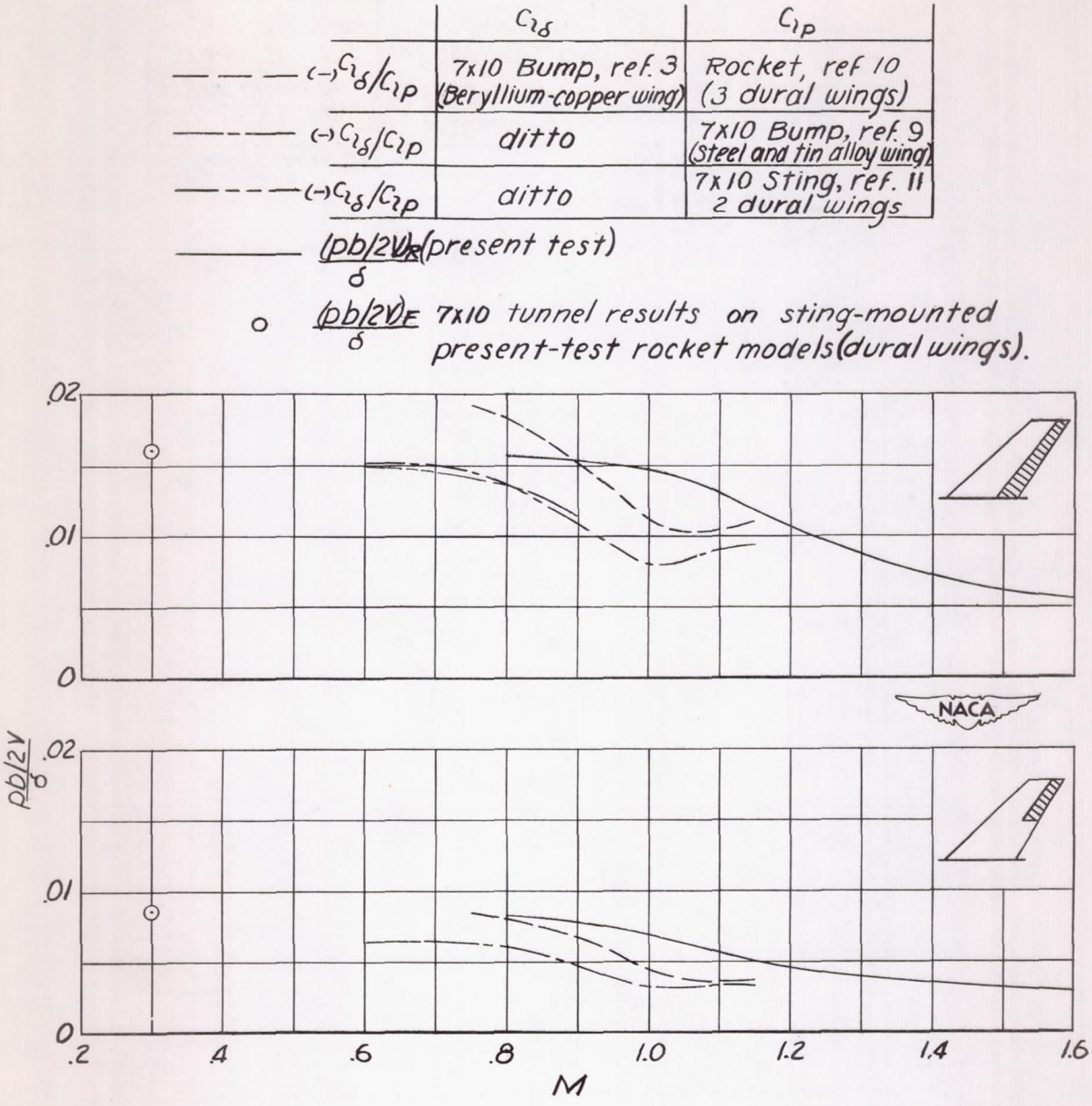

(b) 45° sweptback wings with $0.86\frac{b}{2}$ - span and $0.43\frac{b}{2}$ - span outboard ailerons.

Figure 17.- Continued.

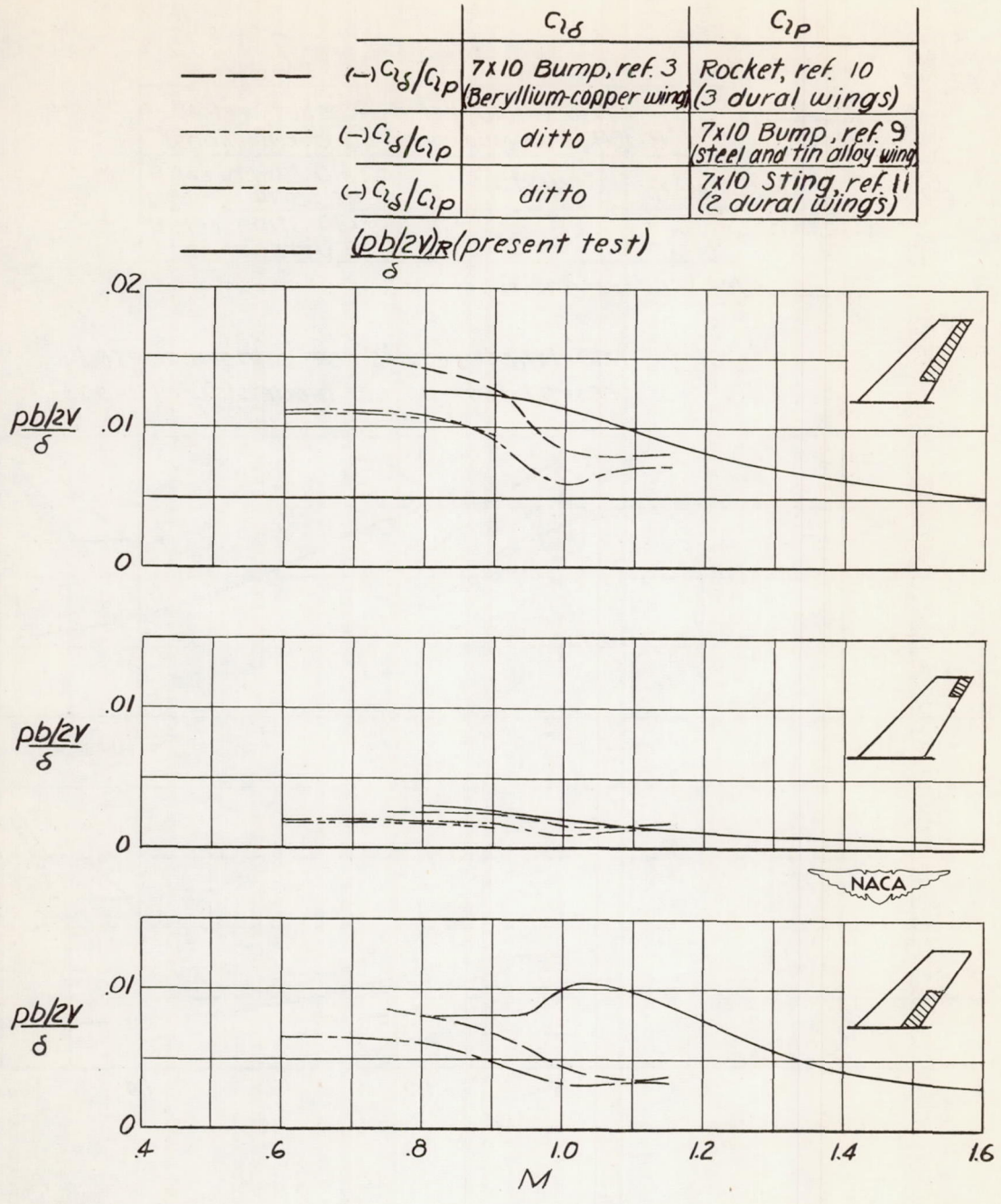

(c) 45° sweptback wings with outboard $0.645\frac{b}{2}$ - span and $0.245\frac{b}{2}$ - span ailerons and inboard $0.43\frac{b}{2}$ - span ailerons.

Figure 17.- Concluded.